Hindawi
Journal of Food Biochemistry
Volume 2023, Article ID 6711132, 21 pages
https://doi.org/10.1155/2023/6711132

Research Article

Exploring the Effects of Solid-State Fermentation on Polyphenols in *Acanthopanax senticosus* Based on Response Surface Methodology and Nontargeted Metabolomics Techniques

Jianqing Su, Xiang Fu, Rui Zhang, Xiaoli Li, Ying Li, and Xiuling Chu

College of Agronomy and Agricultural Engineering, Liaocheng University, Liaocheng 252000, China

Correspondence should be addressed to Jianqing Su; sujianqing@lcu.edu.cn and Xiuling Chu; chuxiuling@lcu.edu.cn

Jianqing Su and Xiang Fu contributed equally to this work.

Received 20 January 2023; Revised 13 May 2023; Accepted 31 May 2023; Published 9 June 2023

Academic Editor: Christophe Hano

In order to optimize the process of solid-state fermentation and understand the changes of active ingredients during fermentation of *A.senticosus*, we used response surface methodology to optimize the solid-state fermentation process of *A.senticosus* and analyzed the effect of fermentation on the active components of *A.senticosus* by nontargeted metabolomics techniques. The effects of fermentation conditions on polyphenol content were studied in terms of fermentation time, fermentation temperature, water content, and the inoculum level through Plackett–Burman design and response surface experiments. The optimized fermentation conditions were a fermentation time of 60 h, a fermentation temperature of 37°C, a water content of 55%, and an inoculum level of 12.5%, and the polyphenol content reached $10.25 \pm 0.05\ \text{mg}\cdot\text{g}^{-1}$, which was 40% higher than that before fermentation. Furthermore, the metabolites and metabolic pathways of *A. senticosus* were analyzed before and after fermentation using nontargeted metabolomics techniques, and differences in metabolites were investigated based on the analysis of the principal components. The results showed that *A.senticosus* contained 57 phenolics, and a total of 12 polyphenolic metabolites were significantly different before and after fermentation (including phenols and isoflavonoids), among which the content of caffeic acid and its derivatives with antioxidant capacity was significantly increased, which may improve the antioxidant capacity of fermented *A.senticosus*. Therefore, solid-state fermentation opens new avenues for the clinical development and application of *A. senticosus*.

1. Introduction

Acanthopanax senticosus Harms is a genus of *Acanthopanax* in the *Acanthopanax* family, and its dried root, rhizome, or stem were used as treatment medicine [1, 2]. It can work to strengthen the body and mind and has the efficacy of nourishing Qi, strengthening the spleen, nourishing the kidney, and soothing the nerves [3]. The primary chemical constituents of *A. senticosus* include polyphenols [4], polysaccharides [5], glycosides [6], and lignans, which have good pharmacological activities to regulating immune function [7], antifatigue effect [8], antioxidant activity [9], and anti-inflammatory properties [10]. Polyphenols are secondary plant metabolites found in traditional Chinese medicine with potential effects on health and are also the general term for plant components with several phenolic hydroxyl groups in the molecular structure, including polyphenols, tannins, phenolic acids, and anthocyanins [11].

As beneficial microorganisms, probiotics play a unique role in physical health, such as improving immunity [12], producing beneficial metabolites [13], and regulating intestinal flora balance [14]. Traditional Chinese medicine uses high-purity single high-purity strain or hybrid strain [15] and can improve active component content and efficacy [16]. Most of the active ingredients in traditional Chinese medicine are found in the cell wall. The cell wall is rich in lignin, cellulose, pectin, and other dense structural components, which increases the hardness of the cell wall and is not easy to decompose, hindering the release of the active ingredients of traditional Chinese medicine from the cell [17]. It has been demonstrated that the traditional

Chinese medicine cell wall can be degraded by various enzymes produced by microorganisms, releasing more active ingredients [14]. Therefore, the content of dynamic components [18] and efficacy of alkaloids [19], saponins, flavonoids, polysaccharides, and organic acids in traditional Chinese medicine will be improved after microbial fermentation and are more suitable as feed additives [20]. With the continuous innovation of microbial fermentation technology and the deepening of the modernization of traditional Chinese medicine, microbial fermentation and transformation of traditional Chinese medicine have aroused great interest and gradually become a new way to produce new active compounds with potential medicinal value.

Nontargeted metabonomics focuses on detecting hundreds of individual compounds rather than identifying or quantifying specific compounds [21]. Metabonomics is widely used to monitor the quality, processing, safety, and microbiology of fermented products. In this study, the previously optimized process parameters were used for the solid-state fermentation of *A. senticosus* (FAS), and the changes in the chemical components of the substrate in the fermentation process were analyzed. Using unfermented *A. senticosus* (AS) as a control, the metabolites of the compound of *A. senticosus* were identified by ultra-performance liquid chromatography and mass spectrometry [22]. The study established chromatographic and mass spectrometric conditions, used partial least squares discriminant analysis to screen compounds, matched the secondary mass spectrometry information with the database, identified related compounds, and obtained the metabolic material spectrum during the fermentation process of *A. senticosus*. Bioinformatic tools and software were used to classify and analyze the identified metabolites, systematically identify the primary metabolites and critical metabolic pathways in the fermentation process of *A. senticosus*, and provide a reference for the application of *A. senticosus*.

2. Materials and Methods

2.1. Reagents and Strains. The *A. senticosus* was purchased from Liaocheng Limin Pharmacy and dried at 60°C in an oven with constant weight. After drying, the plant was crushed with a pulverizer and sieved with 200 mesh. About 1500 g powder of *A. senticosus* was used in the experiment. The powder was stored in a refrigerator at 4°C for subsequent testing. Formic acid was purchased from CNW; 2-Propanol was purchased from Merck; 2-Chloro-L-Phenylalanine was purchased from Adamas-beta. *Lactic-lactobacillus Plantarum*, *Saccharomyces cerevisiae*, and *Bacillus subtilis* were isolated from the intestine of healthy chickens in the laboratory. These strains were identified by routine methods using 16S rRNA and physiological and biochemical tests. These were sourced from laboratory-preserved strains. The concentration of all strains used for fermentation is 1×10^8 CFU/ml, and the addition ratio is 1 : 1 : 1.

2.2. Fermentation of A. senticosus. The *A. senticosus* powder (10 g) was accurately weighed and placed in a conical flask; 10 ml of distilled water and 0.1 g of glucose were added and sealed separately; the sealed conical flask was placed in an autoclave for 30 minutes, taken out, and placed on an ultraclean bench, and it was cooled to room temperature. *Lactobacillus Plantarum*, *Saccharomyces cerevisiae*, and *Bacillus subtilis* were added to their enrichment medium, placed on a shaker, and incubated and treated at 37°C for 24 h. The concentration of bacteria was adjusted to 1×10^8 CFU/mL. The bacteria and *Saccharomyces cerevisiae* were stirred and mixed on the ultraclean bench and placed in a constant temperature incubator for fermentation. After the fermentation was finished, they were baked in a blast dryer until they reached a constant weight and then used for the later experiments.

2.3. Extraction of Polyphenol from A. senticosus and Calculation of Its Content. Dried FAS powder (1.0 g) was weighed. Polyphenols were extracted using the ultrasonic-assisted method (time = 40 min and power = 600 W) with 10 ml of 60% ethanol as the extraction solvent. In this paper, the extraction temperature was 60°C and the solid-liquid ratio was 1 : 30 (g : mL). After that, it was cooled, filtered, and centrifuged at 10,000 rpm^{-1} for 10 minutes to determine the polyphenol content of the supernatant. The content of polyphenol was determined by the Folin–Ciocalteu method described by Pham [23], with gallic acid as the standard. The polyphenol yield of *A. senticosus* (Y) was calculated according to the following equation:

$$Y = \frac{(C \times N \times V)}{M}, \tag{1}$$

where C is the polyphenol content in *A. senticosus*, V is the volume after the extraction, N is the dilution ratio of the sample, and M is the mass of the raw material.

2.4. Optimization by the Response Surface Method. The effects of fermentation time, fermentation temperature, the inoculum level, water content, glucose addition, and urea addition on polyphenol content were first investigated by single-factor tests. Then, a Plackett–Burman design (PBD) was performed, and PBD was usually applied to conduct a minimum number of experiments to assess the relative importance of various parameters. Six factors affecting polyphenol content were selected, including fermentation time, fermentation temperature, inoculum, water content, glucose addition, and urea addition, with polyphenol content (Y) as the response value. A 6-factor 2-level PBD was designed using Design Expert 10 software, with two levels of high (+1) and low (−1) set for each variable (Table 1), and the effect of each variable on polyphenol content was calculated by the difference between the high and low levels of the difference between the mean values. Finally, a Box–Behnken experiment with four factors and three levels was conducted for four screened factors, including water content (A), fermentation time (B), inoculum (C), and fermentation temperature (D), based on the Plackett–Burman results (Table 2). Both Plackett–Burman and BBD experimental designs were generated using Design Expert 10 software.

Table 1: Factors and levels of the Plackett–Burman design.

Trial no.	Levels	
	−1	1
Fermentation time (h)	36	60
Fermentation temperature (°C)	33	37
Inoculation amount (%)	7.5	12.5
Water content (%)	45	55
Glucose addition (g/kg)	5	10
Urea addition (g/kg)	5	10

Table 2: Box–Behnken experimental factors and level.

Factors	Levels		
	−1	0	1
A water content (%)	45	55	65
B fermentation time (h)	36	60	84
C inoculation amount (%)	7.5	12.5	17.5
D fermentation temperature (°C)	33	37	41

2.5. Determination of Antioxidant Capacity. In this study, we investigated the changes in the antioxidant capacity of *A. senticosus* before and after fermentation by measuring the scavenging ability of ABTS [24] and DPPH [25] radicals in *A. senticosus* and their total antioxidant capacity.

2.6. Preparation of Nontargeted Metabonomics Samples. The samples were slowly thawed at a low temperature of 4°C. 50 mg of sample was accurately weighed into a 2 ml centrifuge tube, a 6 mm diameter grinding bead was added, and 400 μl of extraction solution (methanol: acetonitrile = 1 : 1 (v: v)) containing 0.02 mg/mL of the internal standard (L-2-chlorophenyl alanine) was added. The samples were ground for 6 min at −10°C at 50 Hz using a frozen tissue mill, extracted by ultrasonication for 30 min at 5°C at 40 kHz, left to stand at −20°C for 30 min, and centrifuged for 15 min at 13,000 g at 4°C, and the supernatant was removed to an injection vial with an internal cannula for analysis in the machine. Quality control (QC) samples were prepared by mixing the extracts of all models in equal volumes, with each QC sample having the same volume as the sample and treated and tested in the same way as the analytical samples.

2.7. UPLC-MS/MS Assay. The instrumental platform for this LC-MS analysis was an ultrahigh performance liquid chromatography-tandem Fourier transform mass spectrometry UHPLC-Q Exactive system from Thermo Fisher. Chromatographic conditions: the column was an ACQUITY UPLC HSS T3, mobile phase A was 95% water +5% acetonitrile (containing 0.1% formic acid), and mobile phase B was 47.5% acetonitrile + 47.5% isopropanol + 5% water (containing 0.1% formic acid); the flow rate was 0.40 mL/min, the injection volume was 2 μL, and the column temperature was 40°C.

2.8. Statistical Analysis. Box–Behnken experiments were designed using Design-Expert. The 8.0.6 software and Graphpand 8.0 software packages were used to analyze variance (ANOVA) and plot data. Principal component analysis (PCA), cluster analysis, partial least squares discriminant analysis (PLS-DA), and orthogonal partial least squares discriminant analysis (OPLS-DA) were used to predict the stability and reliability of the models. Multidimensional statistical analysis (using VIP values) and one-dimensional statistical analysis (p values) were used to predict the stability and reliability of the models. Metabolites with VIP > 1, $p < 0.05$, FC value > 1, or C value < 1 were selected as differential metabolites. Each group of different metabolites was clustered by hierarchical clustering. Each treatment was carried out in triplicate, and experimental results were expressed as the mean ± standard deviation.

3. Results

3.1. Response Surface Analysis. Using the polyphenol content in the fermentation process produced as an indicator, many factors affecting the fermentation process of *A. senticosus* were screened, and the PBD in Table 1 was fitted and analyzed by ANOVA using Design Expert software. The results are shown in Table 3, and the regression model was highly significant ($p < 0.01$) with a coefficient of determination R2 value of 0.9335, indicating that 93.35% of the variance could be estimated by this equation. Among them, fermentation temperature, fermentation time, inoculum amount, and water content reached significant levels ($p < 0.05$) and were the main effect factors affecting the production of *A. senticosus* polyphenols. A Box–Behnken design (BBD) in response surface methodology (RSM) was selected to determine the optimal fermentation conditions for *A. senticosus*. Based on the experimental results, the polyphenol yield was used as an indicator and four parameters, namely, water content (A), fermentation time (B), inoculation amount (C), and fermentation temperature (D), were selected as variables for optimising fermentation technology. The practical steps, the corresponding experimental results, the experimental design, and the results of the response surface are shown in Table 4.

Herein, A, B, C, and D refer to water content, fermentation time, inoculation amount, and fermentation temperature, respectively. The experimental data were designed and processed by Design Expert 8.0.6 software, and the variance analysis of the regression model was obtained. The results are shown in Table 5. After the quadratic polynomial fitting of the nonlinear regression, the prediction model was obtained as follows:

$$\begin{aligned} Y = {} & 10.26 + 0.18A + 0.24B + 0.08C + 0.39D + 0.07AB \\ & + 0.01AC - 0.02AD - 0.08BC - 0.13BD + 0.01CD \\ & - 0.83A^2 - 0.72B^2 - 1.01C^2 - 1.20D^2. \end{aligned} \quad (2)$$

As shown in Table 5, the proposed mathematical model is significant ($p < 0.0001$), the lack-of-fit term is little ($p > 0.05$), and the corrected coefficient of determination R2 is 0.9545, indicating that 95.45% of polyphenol content of *A. senticosus* can be determined by the model to explain; R2

Table 3: Factor levels and significance analysis of Plackett–Burman.

Source	SS	Df	MS	F-value	p value
Model	10.7	6	1.78	11.7	0.0082
Fermentation time (h)	1.97	1	1.97	12.9	0.0157*
Fermentation temperature (°C)	5.91	1	5.91	38.73	0.0016*
Inoculation amount (%)	1.43	1	1.43	9.38	0.028*
Water content (%)	1.31	1	1.31	8.59	0.0326*
Glucose addition (g/kg)	0.0143	1	0.0143	0.0936	0.7719
Urea addition (g/kg)	0.0748	1	0.0748	0.4908	0.5148
Residual	0.7624	5	0.1525		
Cor total	11.46	11			

Note. SS: sum of squares; DF: degree of freedom; MS: mean sum of squares. *Statistically significant at 95% of the probability level.

Table 4: Response surface design and experimental results.

Number	A	B	C	D	Phenol yield ($mg \cdot g^{-1}$)
1	55	36	12.5	33	7.56
2	55	36	7.5	37	8.00
3	45	36	12.5	37	8.45
4	65	60	12.5	41	8.96
5	65	60	7.5	37	8.36
6	55	36	12.5	41	8.50
7	55	60	12.5	37	10.29
8	55	60	17.5	33	7.44
9	55	60	7.5	41	8.45
10	45	60	7.5	37	8.06
11	55	60	12.5	37	10.50
12	45	60	12.5	33	7.80
13	45	60	17.5	37	8.20
14	45	84	12.5	37	8.48
15	55	84	17.5	37	9.21
16	65	36	12.5	37	8.61
17	65	84	12.5	37	8.95
18	55	84	12.5	41	8.60
19	55	60	12.5	37	10.05
20	55	60	12.5	37	10.17
21	55	84	7.5	37	9.06
22	55	60	17.5	41	8.48
23	45	60	12.5	41	8.56
24	55	60	12.5	37	10.27
25	65	60	17.5	37	8.57
26	55	36	17.5	37	8.50
27	55	60	7.5	33	7.47
28	65	60	12.5	33	8.31
29	55	84	12.5	33	8.20

is 0.9091, demonstrating that the polyphenol content of *A. senticosus* is changed and the equation established is a proper fit for the experiment. The effects of the respective variable factors on the polyphenol content of *A. senticosus* are as follows. The primary factors B (fermentation time) and D (fermentation temperature), A2, B2, C2, and D2 had rather significant effects on the polyphenol yield of *A. senticosus* ($p < 0.01$). The effect of A (water content) on the total polyphenol content of *A. senticosus* was significant ($p < 0.05$). AB (water content and fermentation time), AC (water content and inoculation amount), AD (water content and fermentation temperature), BC (fermentation time and inoculation amount), BD (fermentation time and fermentation temperature), and CD (inoculation amount and fermentation temperature) had no significant effect on the polyphenol content of *A. senticosus* ($p > 0.05$).

The regression analysis results drew the response surface contour map and the response surface three-dimensional map. The three-dimensional map intuitively reflected the effects of the interaction of each factor on the response value, and the optimized parameters and the interaction between the parameters were found. The response surface could be used to evaluate the influence of various factors, with the impact becoming more noticeable as the surface became steeper. Figure 1 illustrates the effects of A, B, C, and D on the polyphenol content of *A. senticosus*. Through the response surface experiment, the optimized process conditions of *A. senticosus* fermentation were determined as follows.

Table 5: Variance analysis and regression coefficient estimation of the response surface.

Source	Sum of squares	Df	Mean square	*F*-value	*p* value	Significant
Model	19.07	14	1.36	20.99	<0.0001	**
A	0.4087	1	0.4087	6.3	0.025	
B	0.6933	1	0.6933	10.69	0.0056	
C	0.0847	1	0.0847	1.31	0.2723	
D	1.91	1	1.91	29.4	<0.0001	**
AB	0.0231	1	0.0231	0.3568	0.5598	
AC	0.0011	1	0.0011	0.0172	0.8974	
AD	0.0026	1	0.0026	0.0408	0.8429	
BC	0.0304	1	0.0304	0.4683	0.505	
BD	0.0729	1	0.0729	1.12	0.307	
CD	0.0009	1	0.0009	0.0145	0.9057	
A^2	4.51	1	4.51	69.46	<0.0001	**
B^2	3.43	1	3.43	52.94	<0.0001	**
C^2	6.73	1	6.73	103.79	<0.0001	**
D^2	9.36	1	9.36	144.36	<0.0001	**
Residual	0.9082	14	0.0649			
Lack of fit	0.7993	10	0.0799	2.94	0.1554	
Pure error	0.1089	4	0.0272			
Cor total	19.97	28				

Note. Y, A, B, C, and D are polyphenol content, water content, fermentation time, inoculation amount, and fermentation temperature, respectively; A2, B2, C2, and D2 are secondary factors of A, B, C, and D, respectively; A.B., A.C., A.D., BC, B.D., and CD are interaction factors.

The fermentation temperature is 37.632°C, the inoculation amount is 12.5%, the fermentation time is 63.562 h, and the water content is 55%. Therefore, the total phenol content in the fermentation broth is predicted to be 10.309 mg/g. Under this condition, the polyphenol content in fermentation products reached 10.25 $mg{\cdot}g^{-1}$, which was 40% higher than before fermentation. After inoculation with the compound strains, during the fermentation process (0~72 d), the total phenol content showed a trend of increasing and decreasing. Yet, the total phenol content reached its highest after the process of fermentation, significantly higher than other samples ($p < 0.05$). In fermentation, microorganisms produced phenols through secondary metabolic pathways and extracellular enzymatic action, and hydrolase was released to hydrolyze complex-bound phenols into monomeric phenol substances, increasing total phenol content [26].

3.2. Free Radical Scavenging Activity of Fermented A. senticosus. DPPH, as one of the few stable organic nitrogen compounds, is often used to evaluate the antioxidant activity of natural antioxidants. The DPPH radical scavenging assay has the advantages of being simple and rapid and can be widely used to determine the antioxidant activity of herbal extracts. Potassium persulfate can oxidize ABTS and produce ABTS radicals with a dark green color, and the scavenging ability of antioxidants on ABTS radicals can be assessed by detecting the decrease in absorbance, so it can be used to test the antioxidant activity of herbal extracts in various media. In this study, the total reducing capacity of *A. senticosus* was also examined based on the assessment of the effect of fermentation on the scavenging capacity of DPPH and ABTS free radicals in *A. senticosus* (Figure 2). The results showed that *A. senticosus* extracts had the scavenging ability for both free radicals and showed a positive correlation with increasing drug concentration. Among them, the IC_{50} values of fermented *A. senticosus* alcoholic extracts (FAS) for the elimination of DPPH and $ABTS^+$ were 0.1764 $mg{\cdot}mL^{-1}$ and 0.6023 $mg{\cdot}mL^{-1}$, which were significantly higher than those of unfermented *A. senticosus* alcoholic extracts (AS). This shows that *A. senticosus* has better in vitro antioxidant ability, and the free radical scavenging ability is stronger after *A. senticosus* fermentation than before fermentation in the concentration range.

3.3. Nontargeted Metabonomic Analysis. Changes in the chemical composition of AS during solid-state fermentation were evaluated using nontargeted metabolomics. In the positive and negative ion modes, the total ion chromatogram is plotted with time as the horizontal coordinate and the intensity of the sum of the ion as the vertical coordinate [27]. Total ion current (TIC) overlap plots from MS analysis of mixed quality control (QC) samples were analyzed by overlap display analysis (Figure 3). The results show a high overlap of the total ion current curves for metabolite detection, indicating a reliable assessment. The metabolites in the samples were extracted and put on the mass spectrometer, and metabolites were detected using both positive and negative ion modes to obtain all of the mass spectrometry data. The metabolites are detected using both anion and cation modes. All mass spectrometry data are obtained, and the mass spectrometry results are imported into the Megi cloud platform for expression data preprocessing. Finally, 939 metabolites were identified in cationic and anionic modes (Table 6). From Figure 4, we can see that for the overall data, when the RSD is less than 0.3, the proportion of the peak is greater than 70%, so it was proven reliable. To better outline and analyze the dynamic changes of metabolites in AS during solid-state fermentation, a heatmap of sample correlations was drawn, where each

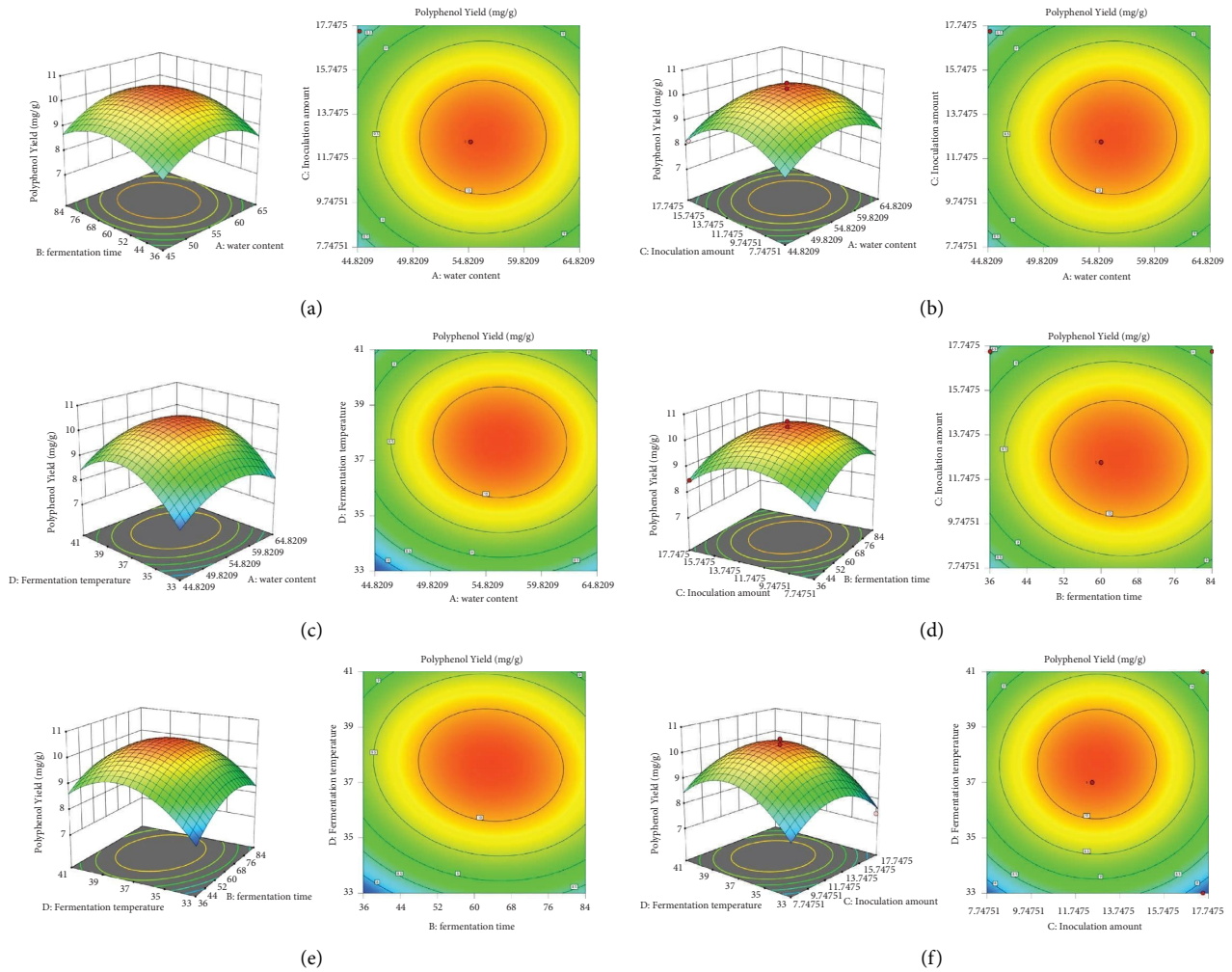

Figure 1: Response surface plots. (a) The effects of water content and fermentation time on the polyphenol yield. (b) The effects of water content and inoculation amount on the polyphenol yield. (c) The effects of water content and fermentation temperature on the polyphenol yield. (d) The effects of fermentation time and inoculation amount on the polyphenol yield. (e) The effects of fermentation time and fermentation temperature on the polyphenol yield. (f) The effects of inoculation amount and fermentation temperature on the polyphenol yield.

grid indicated the correlation between two samples, different colors represented the relative magnitude of correlation coefficients between samples, and the length of clustered branches indicated the close distance between samples [28]. The experimental results confirmed the high repeatability and reproducibility of the data throughout the analysis.

3.4. Multivariate Analysis. To scientifically identify the differences in the accumulation of metabolites between FAS and AS, a metabolite analysis of AS was performed using LC-MS and multivariate analysis. Principal component analysis (PCA) can classify the samples and help us grasp the overall situation of metabolites in FAS and analyze the differences between FAS and AS under optimal fermentation conditions [29]. As shown in Figure 5, parallel samples of the two groups of AS samples, as well as the quality control (QC) sample group, were clustered together, indicating that all assays had good analytical stability and experimental reproducibility; meanwhile, the first principal component (PC1) and the second principal component (PC2) of cations and anions explained 37.20%, 45.50%, 23.00%, and 18.50%, respectively. The cumulative contribution of both reached 60.20% and 64.00%, respectively, which showed a more pronounced separation trend of FAS and AS, reflecting the metabolite differences among these samples.

By appropriately rotating the principal components, the observed values between the groups could be effectively distinguished, and the influencing variables that led to the differences between the groups could be found. After the PLS-DA model was established, if the values of the model parameters (R2 and Q2) were high, the current PLS-DA model was successfully constructed. A substitution test was also conducted for the model parameters R2 and Q2 200 times [30]. The PLS-DA score plots and the results of the replacement test for the samples of AS before and after fermentation are shown in Figure 6. The results are similar to those of PCA. The results show that the R2 and Q2 values of

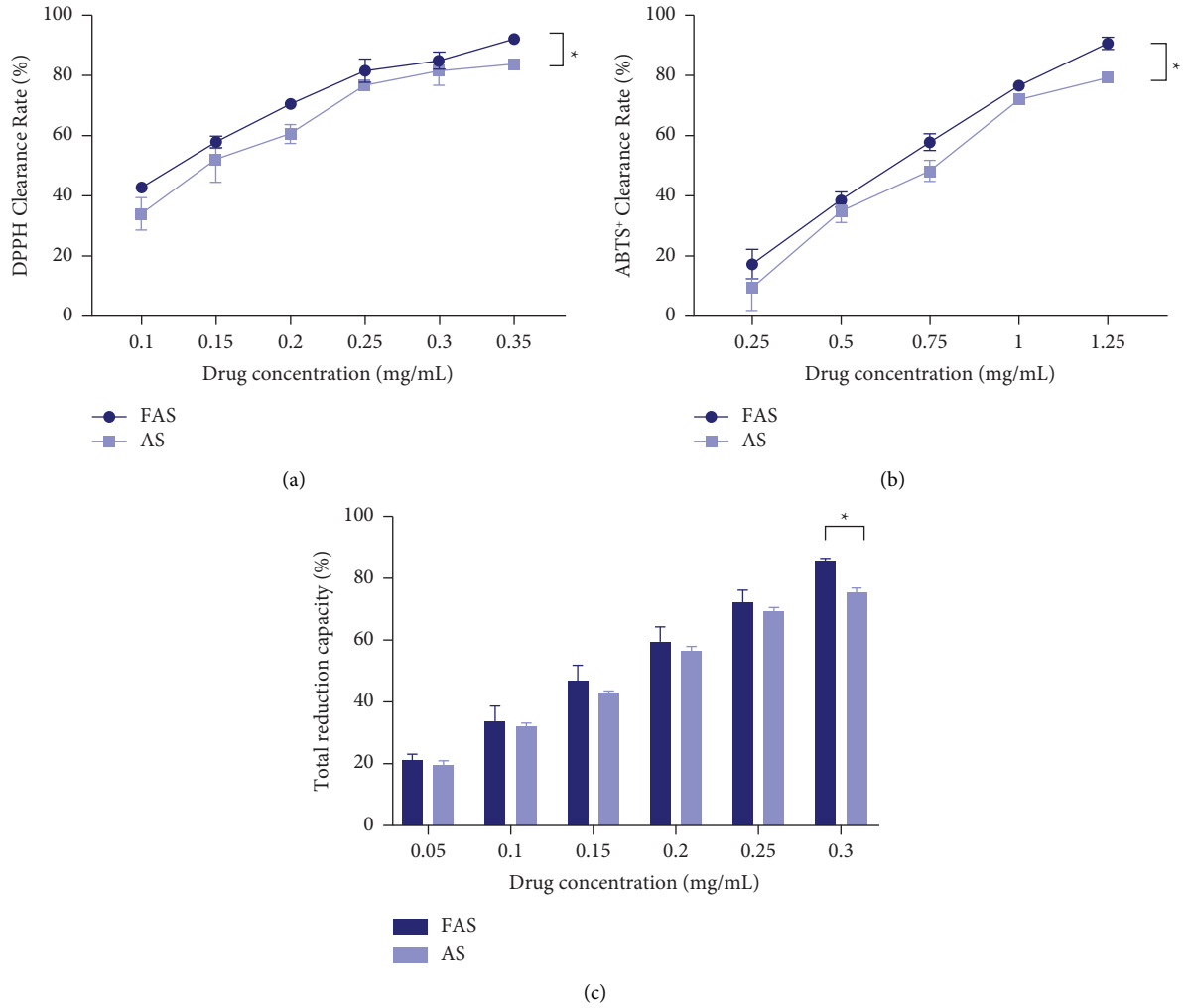

Figure 2: The antioxidant test of Acanthopanax before and after fermentation. (a) Scavenging activity of ABTS radicals, (b) scavenging activity of DPPH radicals, and (c) total reduction capacity. Note: Values are the mean ± standard deviation; *significant differences are at the 5% level.

anions and cations reached above 0.95, indicating that the PLS-DA model was successfully constructed and the replacement test was passed. The model was not overfitted and had good stability and predictability, which can further explore the fermentation process of AS. The model has good stability and predictiveness to further explore the metabolite differences in the fermentation process.

3.5. Identification of Metabolites. The secondary mapping of metabolites matched the secondary mapping of standards in the public database. The statistical results of the classification of the substances identified at the secondary level according to the classification information in the HMDB database are shown in Figure 7 [31]. The results showed that 236 metabolites corresponded to lipids and lipid-like molecules, 103 metabolites corresponded to organic acids and derivatives, 65 metabolites corresponded to organic oxygen compounds, 57 metabolites corresponded to organoheterocyclic compounds, 53 metabolites corresponded to benzenoids, and 53 metabolites corresponded to phenylpropanoids and polyketides. The results showed that the main metabolites of AS were 601 metabolic components after fermentation, of which 57 were phenolic substances, including phenols, cinnamic acids and derivatives, and flavonoids.

The KEGG pathway to which the metabolites were matched was classified, with the vertical coordinate being the secondary classification of the KEGG metabolic pathway, and the horizontal coordinate being the number of compounds annotated to the pathway. The results showed that 522 metabolites were involved in the metabolic pathway, among which 225 metabolites were categorized into metabolism-related pathways, accounting for 43%, as shown in Figure 8(a). Finally, pathway analysis was performed on the metabolites identified at the secondary level, and the identified metabolites were submitted to the KEGG website for metabolic pathway analysis [32]. The results are shown in Figure 8(b). The horizontal coordinates are the top 20 pathways listed, and the vertical coordinates are the number of metabolites matched to the KEGG database. The results showed that 17 metabolites were enriched in the biosynthesis of phenylpropanoid-related pathways and 16 were

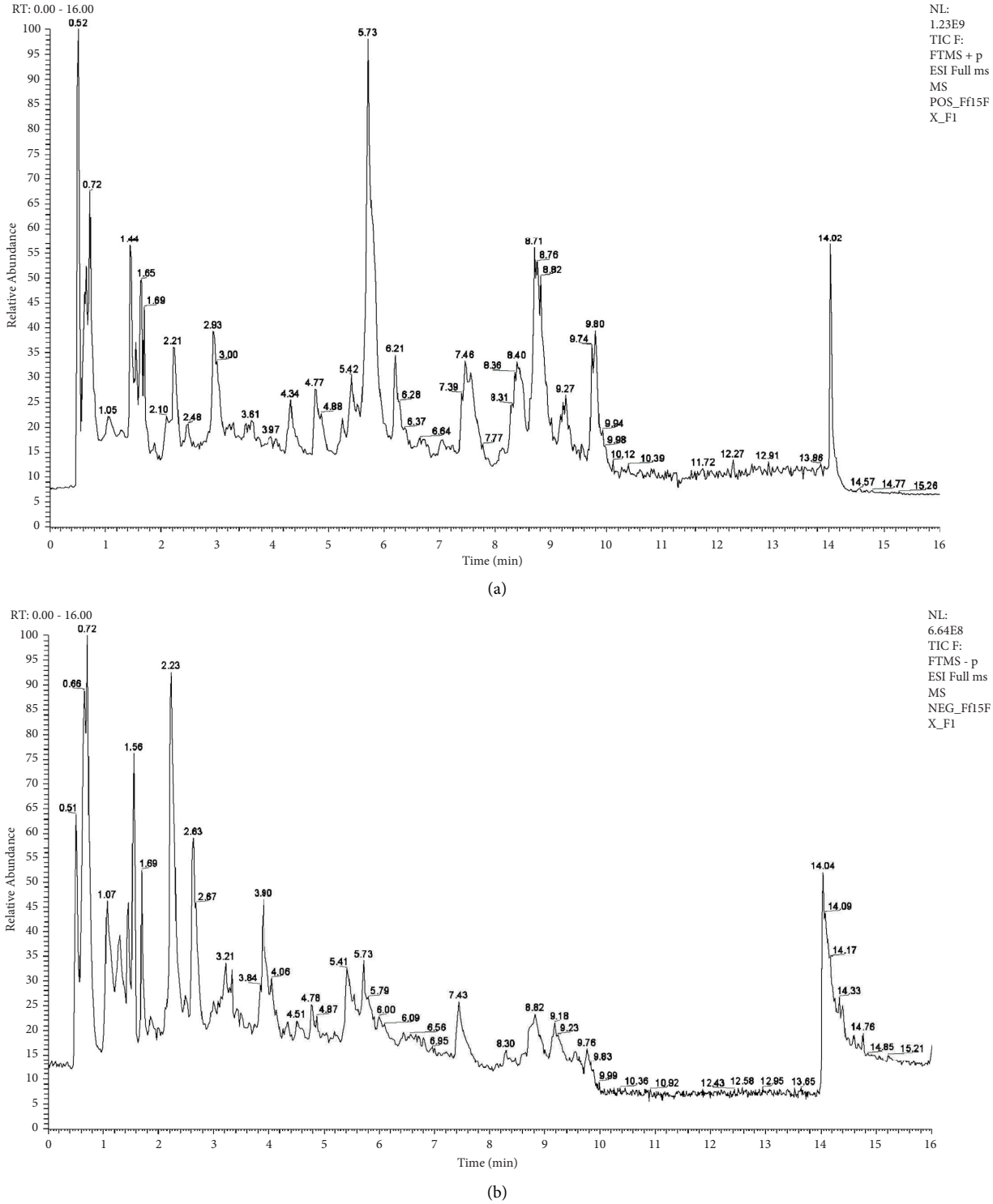

Figure 3: The total ion chromatograms of quality-control samples in positive and negative ion modes. (a) Total ion chromatographic in the cationic mode (positive ion). (b) Total ion chromatographic in the anionic mode (negative ion).

Table 6: Total ion count and identification statistics.

Ion mode	All peaks	Identified	Metabolites	Metabolites
Pos	8976	564	406	192
Neg	8831	375	258	106

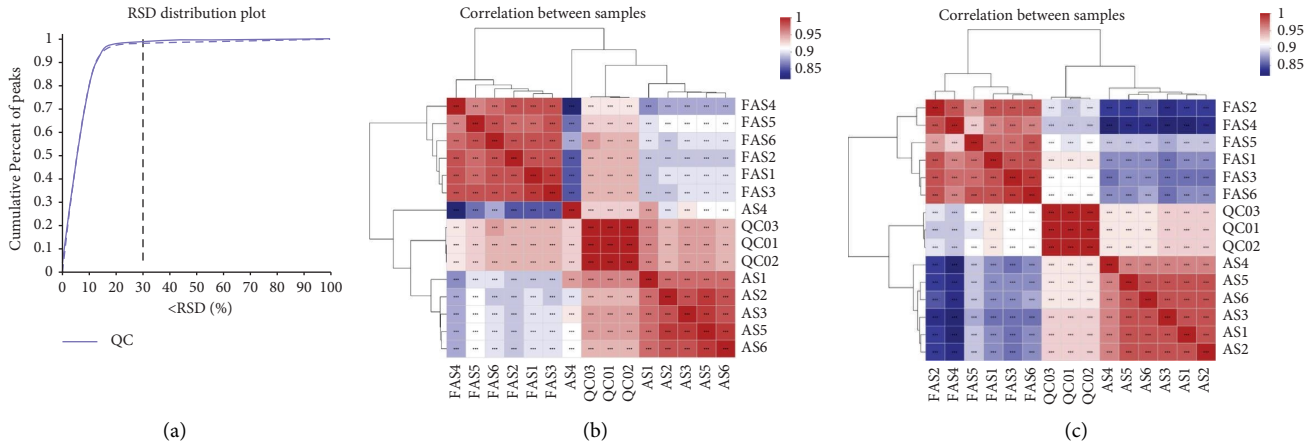

(a) (b) (c)

Figure 4: Correlation among samples. (a) Sample evaluation. (b) The sample correlation heatmap in the cationic mode (positive ion). (c) The sample correlation heatmap in the anionic mode (negative ion).

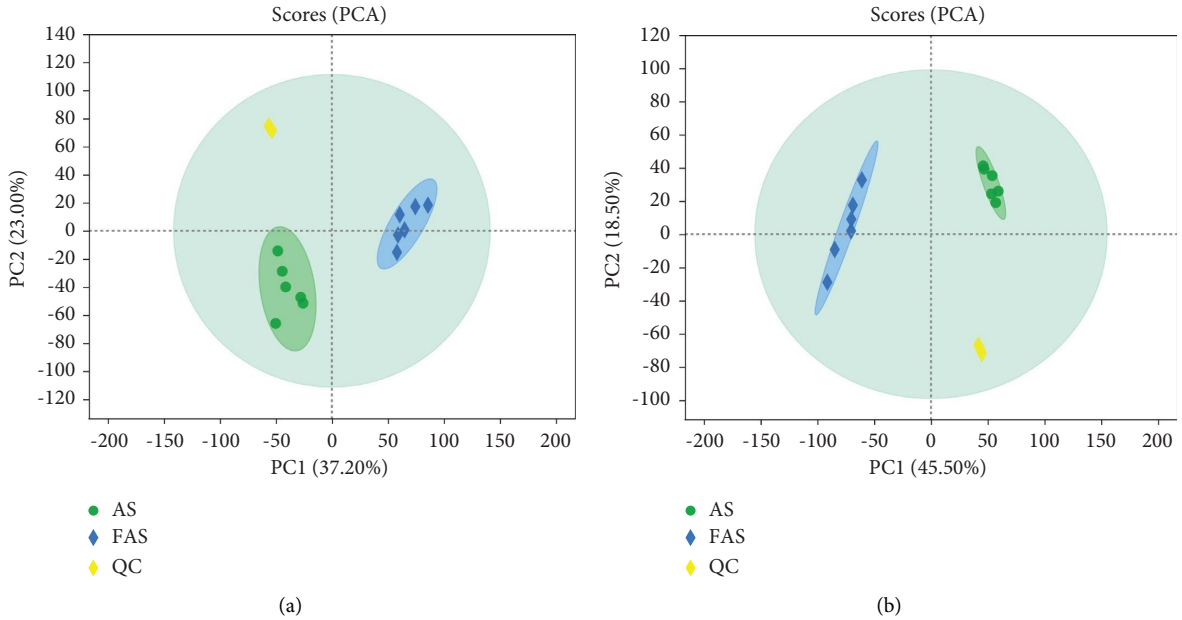

(a) (b)

Figure 5: PCA score plots of different samples. (a) PCA score plots of two groups in the cationic mode (positive ion). (b) PCA score plots of two groups in the anionic mode (negative ion). The confidence ellipse indicates that this group's "true" samples are distributed within this region at a 95% confidence level; beyond this region, the samples are considered possible outliers.

enriched in the biosynthesis of plant secondary metabolite-related pathways. In addition to these metabolites, various amino acid-related metabolic pathways such as alanine, aspartate, and glutamate were involved.

3.6. Identification and Analysis of Differential Metabolites

3.6.1. Differential Metabolite Statistics and OPLS-DA Analysis. The S-plot of the PLS-DA model for the FAS and AS groups in the anion model is shown in Figure 9, where the points further from the origin indicate a more significant contribution to the difference between the groups and their VIP values [33]. In this experiment, metabolites that satisfy both VIP > 1 and t-test $p < 0.05$ were screened as differential metabolites. Two hundred thirty-eight differential metabolites were screened in the metabolites of the FAS and AS groups. Among them, the down-regulated metabolites in the FAS and AS groups compared with each other are indicated by blue dots, red dots indicate the up-regulated metabolites, and the unchanged metabolites are indicated by gray dots (Figure 10).

3.6.2. Cluster Analysis of Differential Metabolites. The metabolite distribution can be visually divided into up-regulation and down-regulation. To directly observe the trend of the concentration of the different metabolites before and after fermentation, a heatmap was made based on the relative content of each different metabolite [34], as shown

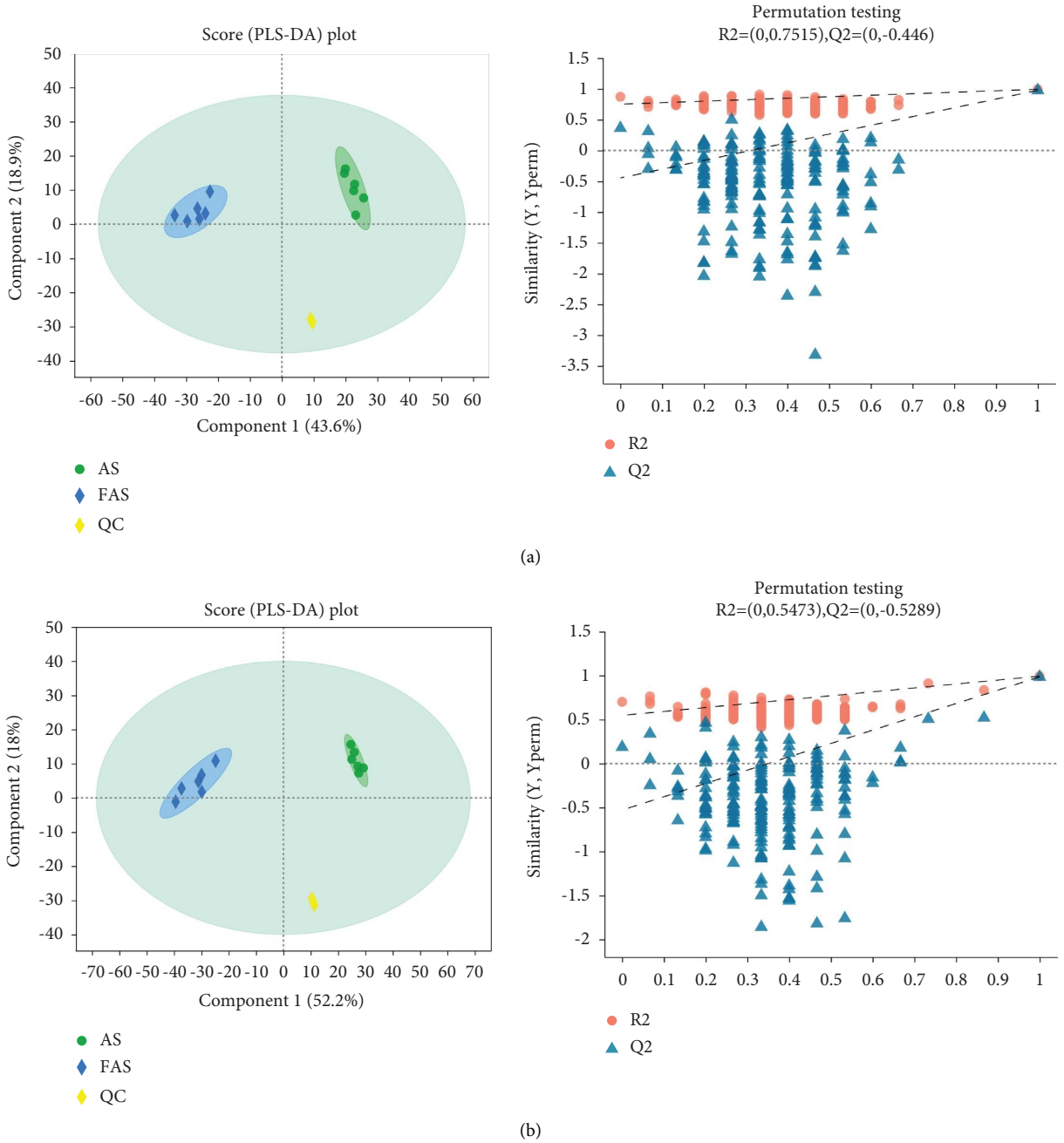

Figure 6: The OPLS-DA model and permutation testing. (a) PLS-DA score plots of two groups in the cationic mode (positive ion). (b) PLS-DA score plots of two groups in the anionic mode (negative ion).

in Figure 11. The tree diagram of the clustering is shown on the left side, and the names of metabolites are shown on the right side. The expression profiles of metabolites in each sample in the FAS and AS groups were the same, the aggregation effect was good, and the high and low expression metabolites could be distinguished. The figure shows that the high content of differential metabolites in the fermentation group (FAS) was more than 75%, which was significantly more than that in the control group (AS), where the content of organic acids and their substituted derivatives and amino acids and their derivatives in the fermentation group was higher than that in the unfermented group. Phenolic substances are essential for plant extracts with vigorous antioxidant activity.

Phenols are a large group of secondary metabolites with diverse structures that are widely distributed in plants. Some polyphenols have a variety of structures, some of which have important pharmacological activities such as antioxidants and anti-inflammatory substances. They can also modify the palatability of fermented herbal medicines and broaden the avenues of application. To better visualize the differential phenolic metabolites, violin plots were used to compare the

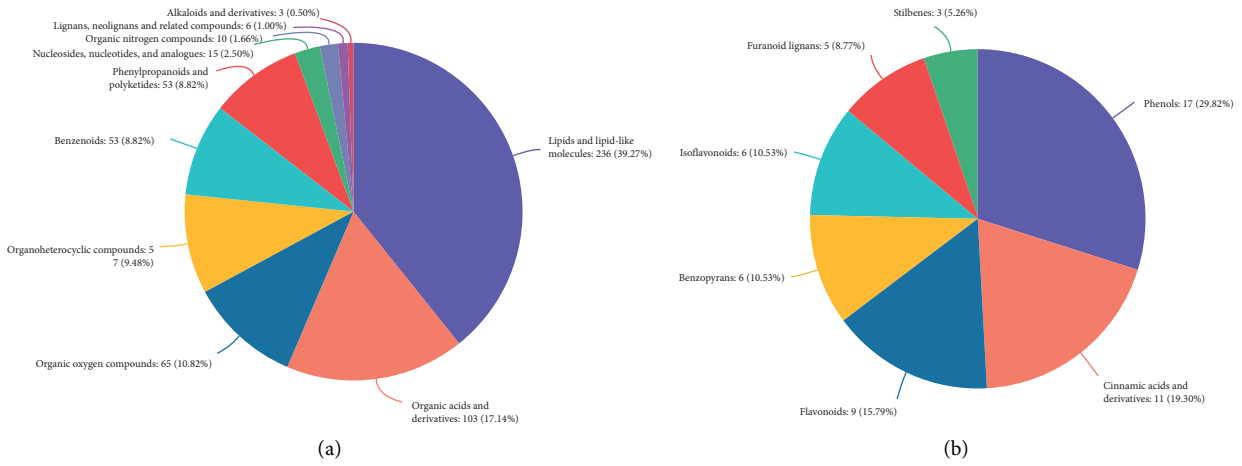

Figure 7: HMDB classification of metabolites. (a) HMDB classification of total metabolites. (b) HMDB classification of phenolic metabolites.

differences in the abundance of phenolic differential metabolites in AS before and after fermentation (Figure 12). Caffeic acid is a natural phenolic acid compound that is widely found in herbal medicines and has antiviral, antioxidant, and antibacterial effects. Lignans are a class of natural lignans, which are plant secondary metabolites that are widely found in nature with rich structural variations and diverse biological activities. The expression of caffeic acid and its derivatives was significantly higher in the FAS group than in the AS group, which may be the reason for the improved antioxidant capacity in the FAS group [35]. Related studies have shown that in the fermentation system, with the action of microorganisms, the enzymes produced can break down bound phenolic acids into free phenolic acids, thus increasing the antioxidant activity and bioavailability of phenolic acids in *A. senticosus*, which may be the reason for the significant increase in the content of free phenolic acids such as cinnamic acid and caffeic acid in *A. senticosus*.

3.7. Metabolic Pathway Analysis of Differential Metabolites. The plant growth process is a very complex metabolic process that must be regulated by a variety of substances and reactions together. The overall judgment cannot be made only from the content of a certain substance, so further analysis of its metabolic pathways is needed. By comparing with the KEGG database, the metabolic pathways involved in the metabolites can be known to evaluate their effects on the biological metabolic process [36]. Forty-one metabolic pathways in 7 categories were retrieved before and after the fermentation of AS. The secondary classification names of KEGG, as shown in Figure 13, were amino acid metabolism, polysaccharide biosynthesis, metabolism, biosynthesis of other secondary metabolites, nucleotide metabolism, carbohydrate metabolism, xenobiotic biodegradation and metabolism, cofactor, vitamin metabolism, another amino acid metabolism, lipid metabolism, terpenoid, polyketide metabolism, exogenous biodegradation and metabolism, carbon metabolism, and various systemic pathways.

Differential metabolites identified during the fermentation of *A. senticosus* were analyzed, and enrichment analysis and topology analysis of metabolic pathways were performed based on the data from the pathway. First, differential metabolites were present in 202 metabolic pathways based on the analysis, among which 99 pathways were significantly aggregated ($p < 0.05$). The most significant key metabolic pathways were selected based on the p value and impact values (Table 7), which were as follows: (1) alanine, aspartate, and glutamate metabolism, including L-asparagine; (2) pyrimidine metabolism, including uracil; (3) arginine and proline metabolism, including L-arginine; (4) tyrosine metabolism, including gentisic acid; (5) citrate cycle (TCA cycle), including malic acid; (6) phenylpropanoid biosynthesis, including caffeic acid; (7) arginine biosynthesis, including L-aspartic acid; (8) valine, leucine, and isoleucine biosynthesis, including 2-isopropylmalic acid; and (9) pyruvate metabolism, including 2-isopropylmalic acid. Figure 14 shows the pathway enrichment diagram, and the experiment was conducted to investigate the effect of fermentation on the analysis of metabolic pathways in *A. senticosus* by analyzing the differential metabolites of *A. senticosus* before and after fermentation. As shown in Figure 14(b), the synthesis of secondary metabolites and phenylpropanoid biosynthesis were dark and significant, which confirmed the significant effect of fermentation on phenolics (e.g., caffeic acid and 2-hydroxycinnamic acid) in *A. senticosus*. Analyzing the role that differential metabolites play in the biosynthesis of secondary metabolites, Figure 15 shows the metabolic pathways associated with differential metabolites, of which four pathways, namely, flavonoid biosynthesis, flavonoid and flavonol biosynthesis, anthocyanin biosynthesis, and isoflavone biosynthesis, are associated with multiple metabolites. Existing studies have shown that the precursors of plant polyphenols are derived from intermediate products of sugar metabolism and synthesized via the phenylpropane metabolic pathway and the flavonoid metabolic pathway, in which most phenolic acids are synthesized via the phenylpropane

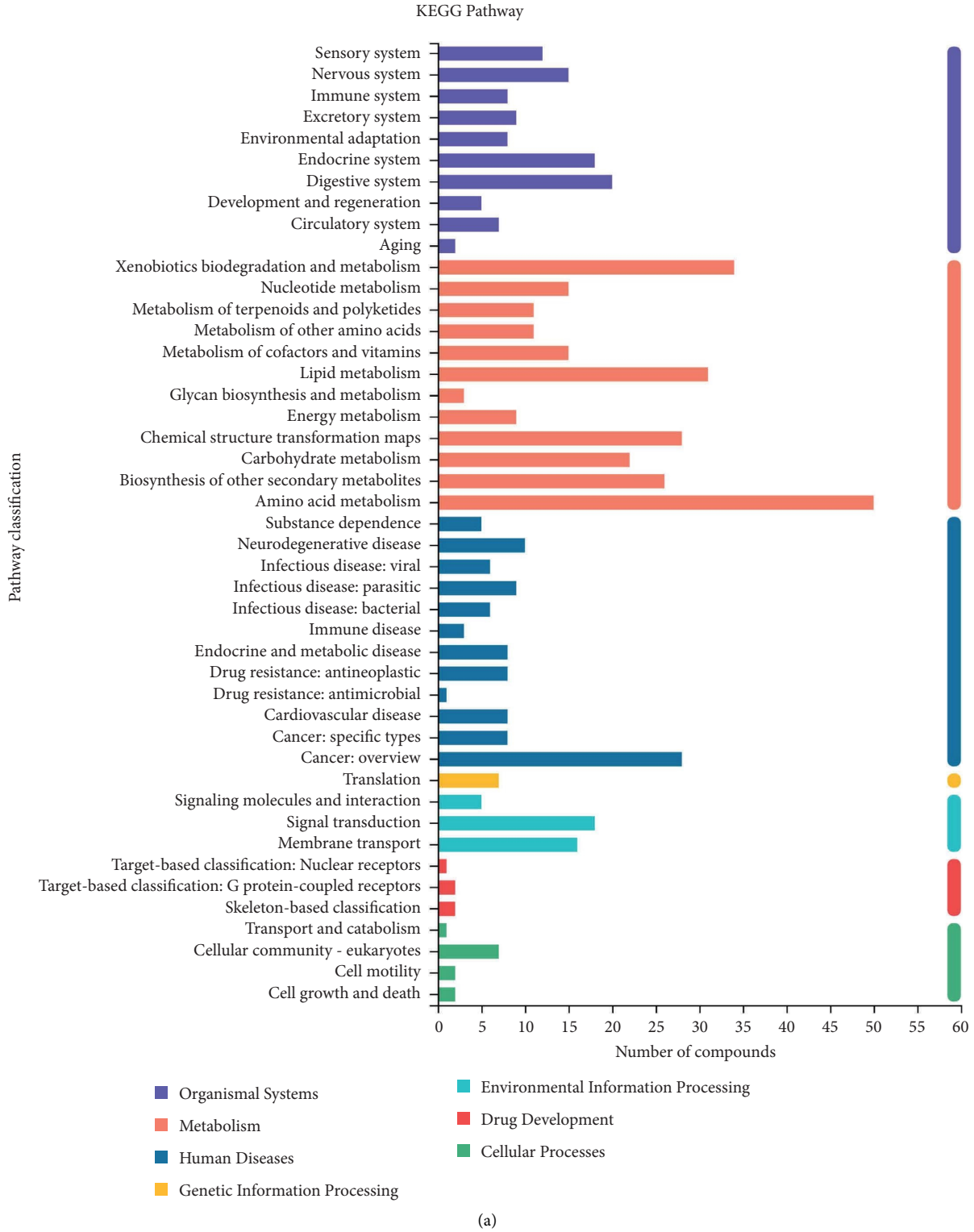

(a)

Figure 8: Continued.

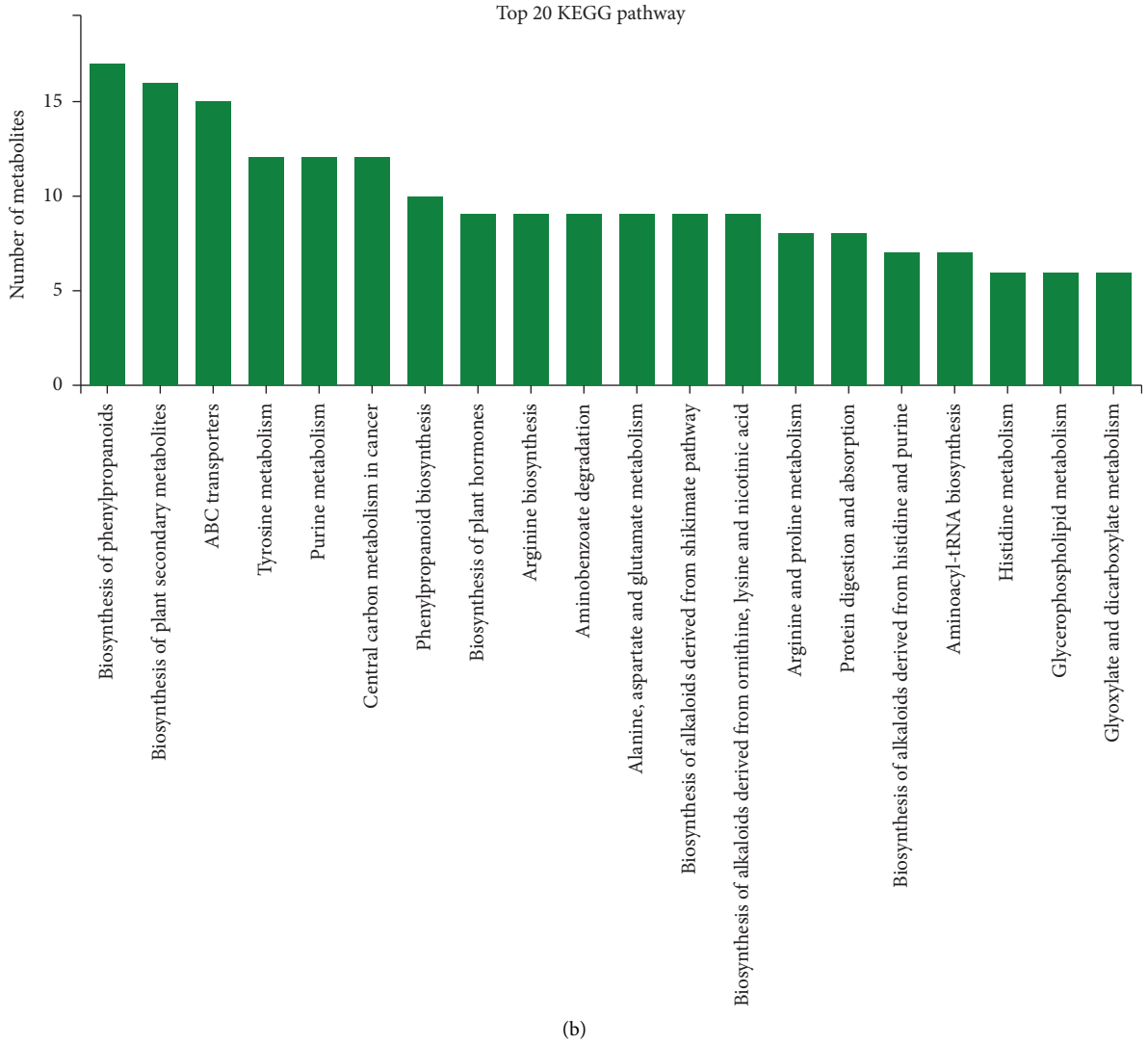

(b)

Figure 8: The metabolic pathway diagram. (a) KEGG pathway classification. (b) Top 20 KEGG pathways involved in secondary identification of metabolites.

metabolic pathway. The phenylpropane metabolic pathway is one of the important secondary metabolic pathways for the synthesis of lignin and flavonoid substances in plants. The phenylpropane metabolic pathway was enriched in this study, which confirmed that fermentation could promote the production of phenolic substances and provide a reference for the effect of fermentation on phenolic substances in Acer sativa.

4. Discussion

In recent years, research on Chinese medicine has become a hot spot for improving the utilisation rate of Chinese medicine and developing new avenues of application. Fermentation is a biochemical reaction process that uses the metabolic function of microorganisms and plant cells to break down organic matter [37]. After microbial fermentation, Chinese medicines can significantly enhance their efficacy, reduce toxicity, and produce new active ingredients. Various studies have shown that fermented Chinese medicines have good effects in promoting growth and development of the body and preventing diseases [38–42]. The strains used in this study were all commonly used probiotics, which produce metabolites beneficial to the host during the fermentation process [43]. Compared with the single strain, the composite strain improved the fermentation efficiency and fermentation quality due to the combined effect of bacteria and enzymes. After the microbial fermentation of *A. senticosus*, the extracellular enzymes such as cellulase and pectinase produced by microorganisms caused its cells to rupture, allowing the precipitation of the active ingredients of *A. senticosus*.

Response surface methodology is an effective method to study the interaction of different factors in the fermentation process. In this study, PBD and BBD experiments were used to determine the optimal fermentation conditions for *A. senticosus*, using the polyphenol content as an experimental index. Polyphenols are a class of secondary

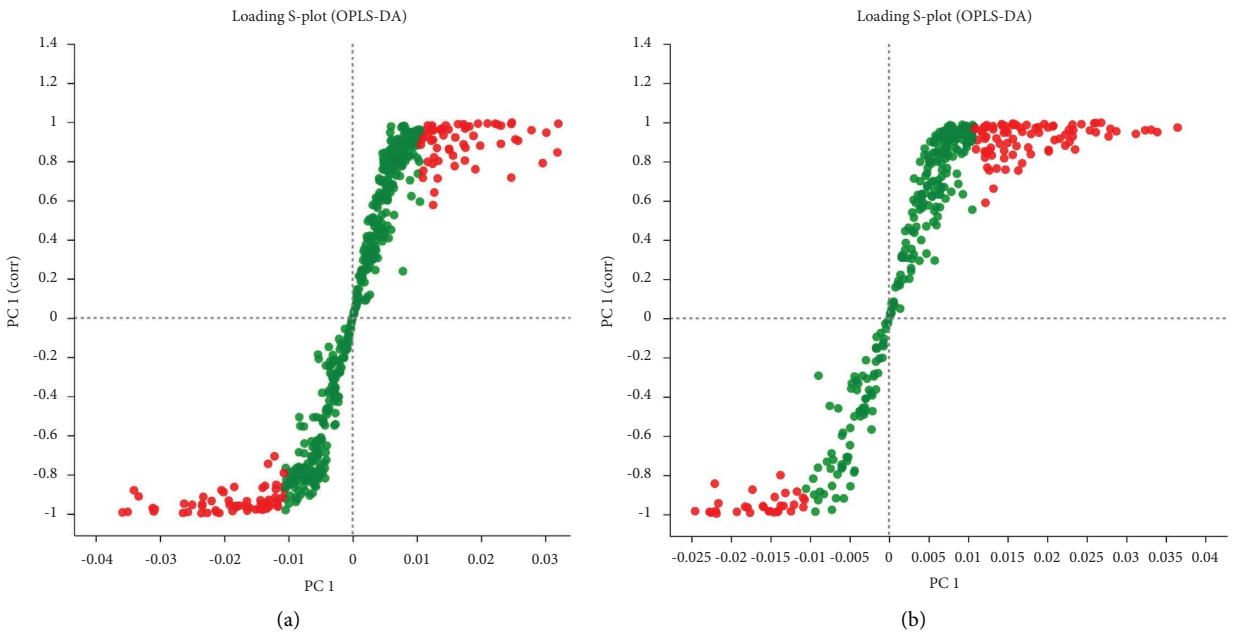

Figure 9: The S-plot of FAS and AS. (a) Cationic mode (positive ion). (b) Anionic mode (negative ion).

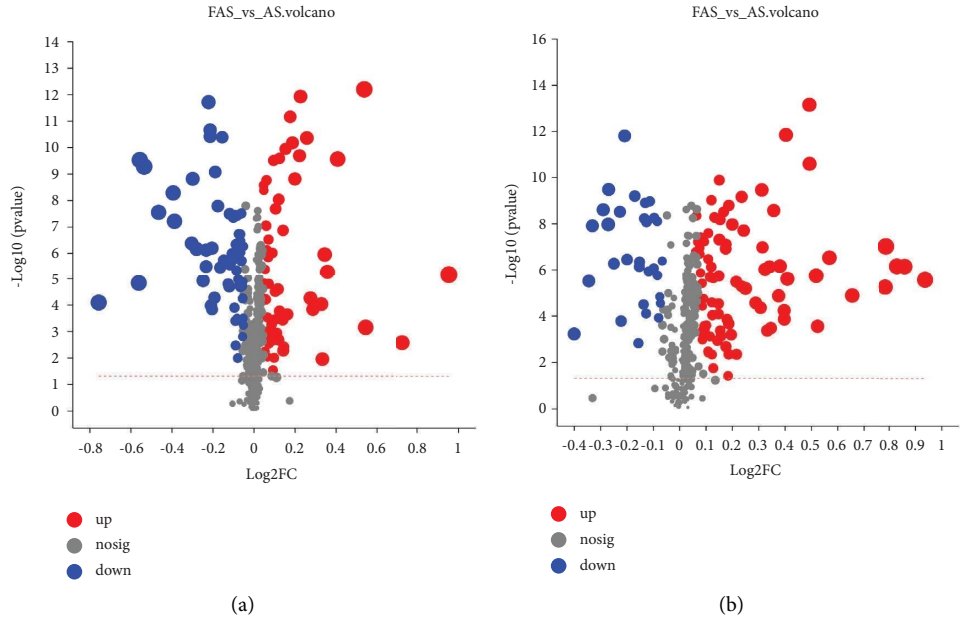

Figure 10: FAS vs. AS different metabolite volcano map. (a) Cationic mode (positive ion). (b) Anionic mode (negative ion).

metabolites widely found in plants. Polyphenol compounds can be covalently bonded with carbohydrates, proteins, and other biological macromolecules to form insoluble bonded polyphenols. During the fermentation process, microorganisms can produce carbohydrate hydrolases such as cellulase, which decompose carbohydrates bound with polyphenols and promote the release of insoluble bonded polyphenols, thus increasing the polyphenol content.

Fermentation time affects the quality of fermentation. As the fermentation time increases, the microorganisms consume nutrients to add value, which in turn increases the active ingredient of the drug [44]. The polyphenol content in this study showed a trend of increasing and then decreasing, which may be because, at the beginning of fermentation, the carbohydrate hydrolase produced by microorganisms promoted the release of insoluble bonded polyphenols, leading to an increase in the polyphenol content; the gradual decrease in the polyphenol content at the later stage of fermentation may be because the release of insoluble bonded polyphenols was complete, while the content was reduced due to the poor stability of polyphenols. The optimal fermentation time for pharyngitis tablet residue prepared by

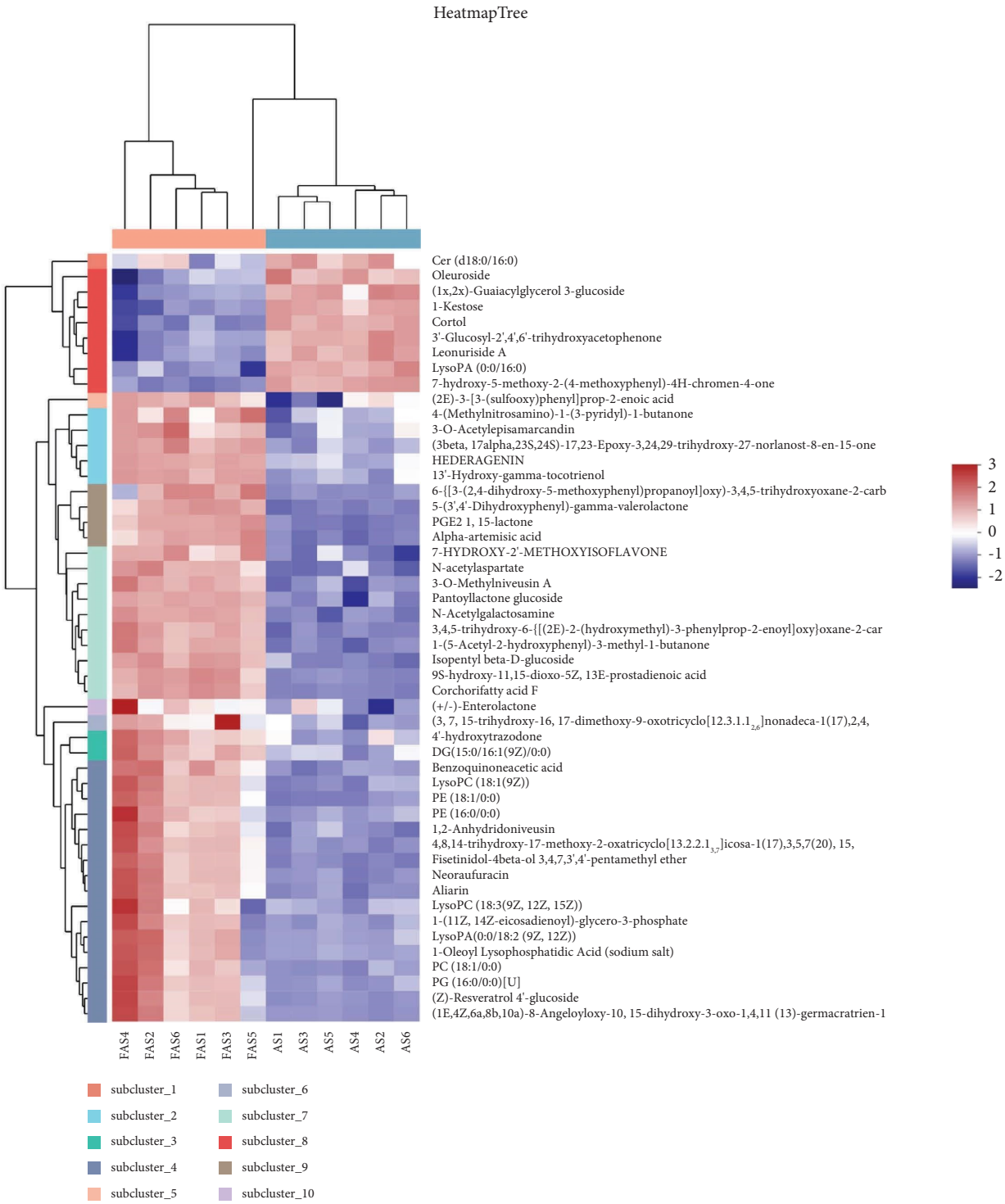

(a)

Figure 11: Continued.

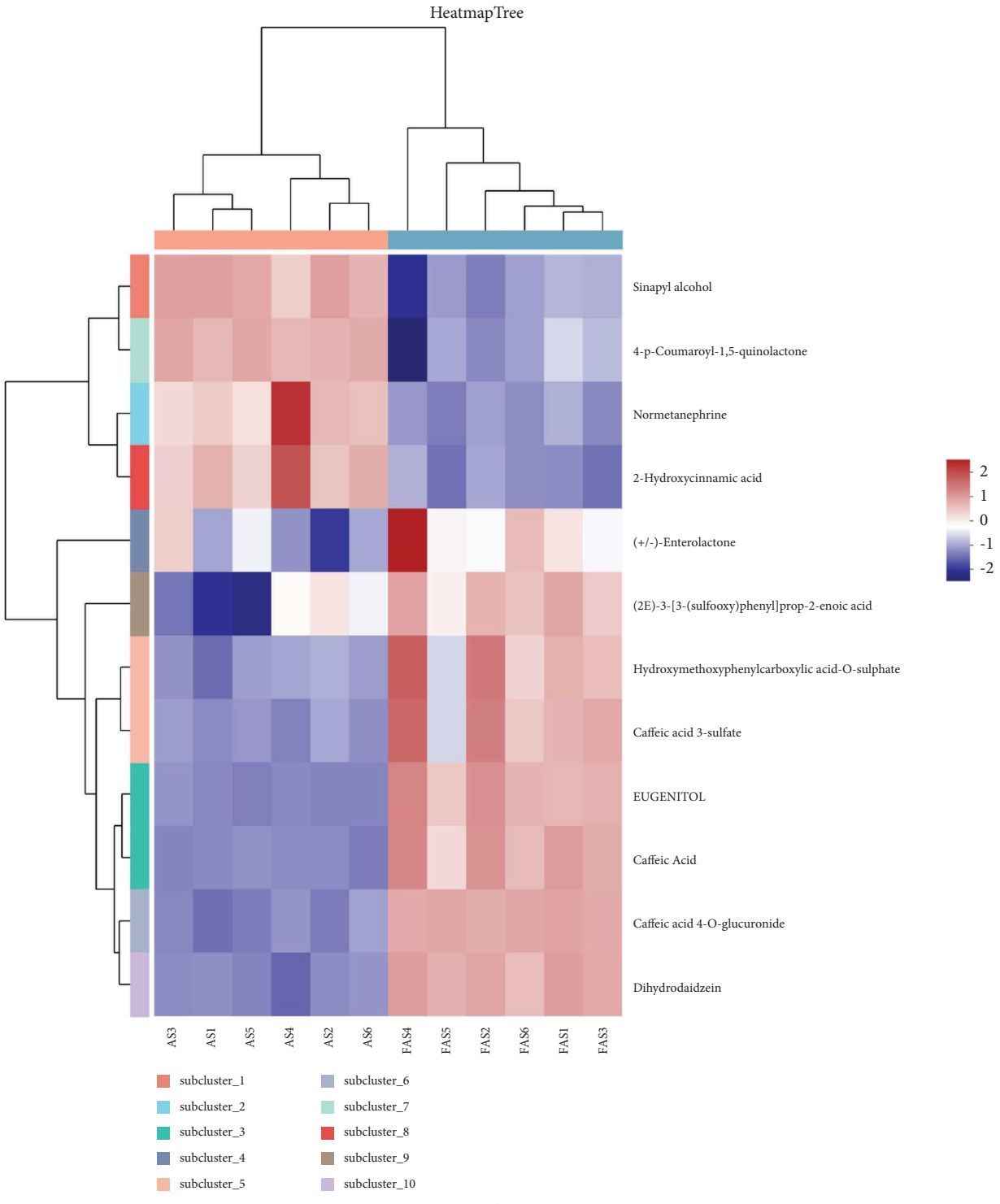

(b)

Figure 11: The heatmap of differential metabolites. (a) Total differential metabolite. (b) Phenol differential metabolite.

other researchers using Lactobacillus Planta-rum and Bacillus subtilis was 72 h [45], while the optimal fermentation time in this study was 60 h, which may be due to the different species of fermentation substrate and inoculated strains.

The water content will also have an important effect on the polyphenol content. Microbial pregrowth, cellulase secretion, transfer, and action all need a certain amount of water to participate, but the increase in water content will lead to the increase in viscosity of the fermentation material and reduce the air exchange, and the waste gas from growth and metabolism will affect the normal growth of the strain. Studies have shown that, at 40–60% water content in solid-

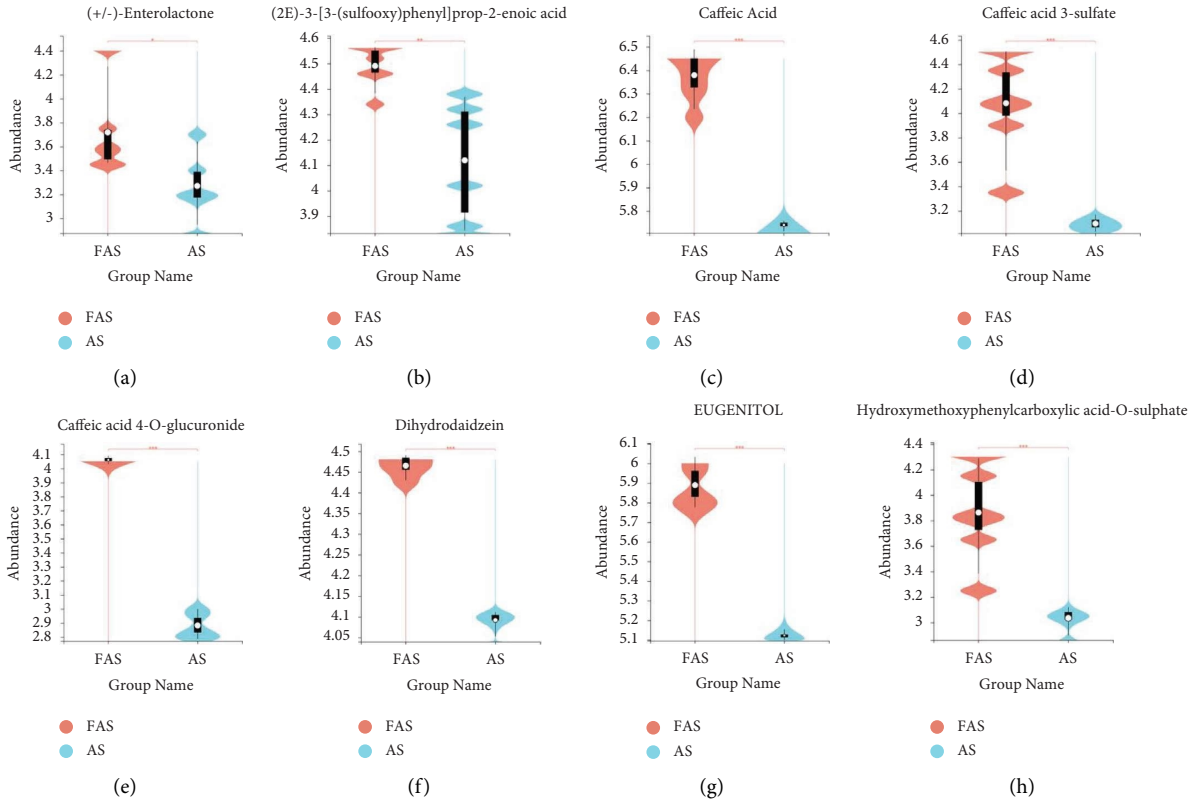

Figure 12: The relative contents of major differential metabolites. (a) (±)-Enterolactone. (b) (2E)-3-[3-(sulfooxy) phenyl] prop-2-enoic acid. (c) Caffeic Acid. (d) Caffeic acid 3-sulfate. (e) Caffeic acid 4-O-glucuronide. (f) Dihydrodaidzein. (g) EUGENOL. (h) Hydroxymethoxyphenyl carboxylic acid-O-sulphate. Note: On the upper side, *represents $p < 0.05$, **represents $p < 0.01$, and ***represents $p < 0.001$.

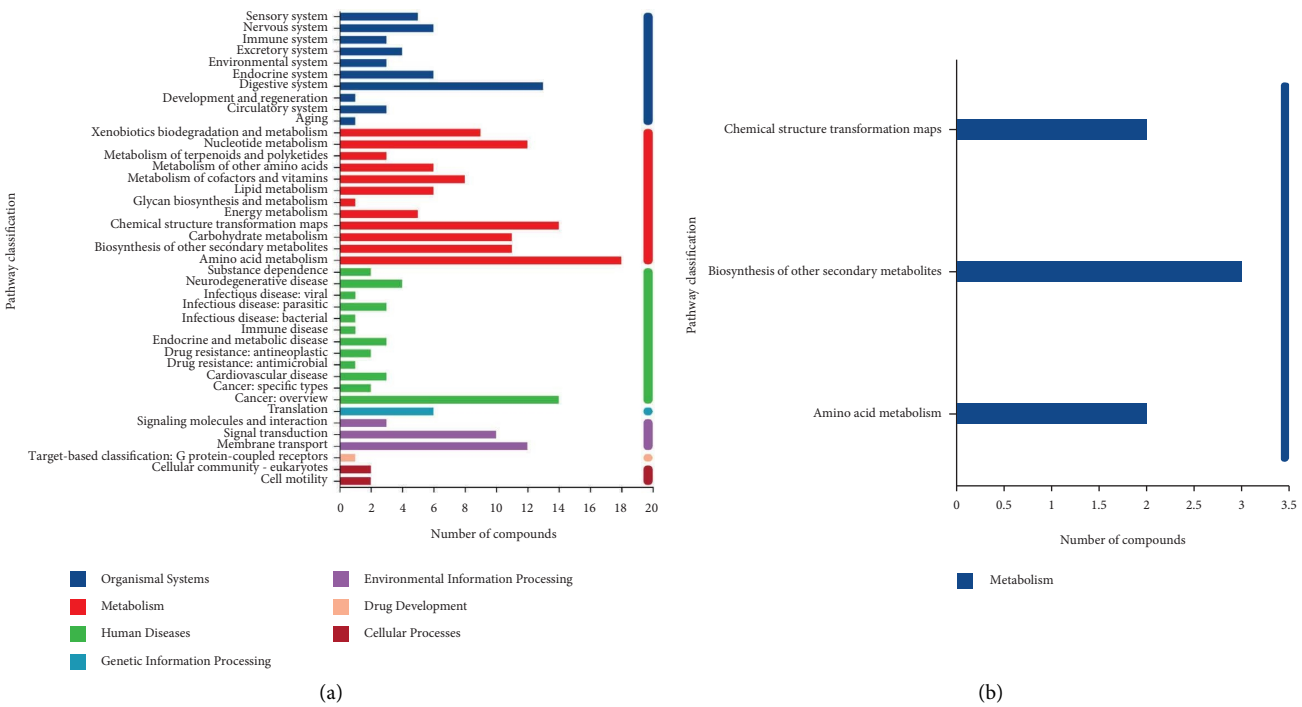

Figure 13: KEGG functional pathway statistics.

Table 7: Analysis of critical metabolic pathways of AS and FAS.

Pathway description	Pathway ID	Match status	Impact value	p value uncorrected	p value corrected
Alanine, aspartate, and glutamate metabolism	map00250	5|28	0.55	0.00000981	0.000239
Pyrimidine metabolism	map00240	5|62	0.22428	0.000460605	0.005173
Arginine and proline metabolism	map00330	3|72	0.200587	0.038940361	0.142132
Tyrosine metabolism	map00350	4|60	0.146438	0.003706591	0.030065
Citrate cycle (TCA cycle)	map00020	2|20	0.120419	0.020401536	0.106379
Phenylpropanoid biosynthesis	map00940	5|62	0.110757	0.000460605	0.005173
Arginine biosynthesis	map00220	4|23	0.105263	0.0000988	0.001443
Valine, leucine, and isoleucine biosynthesis	map00290	3|23	0.102353	0.001968252	0.01796
Pyruvate metabolism	map00620	2|28	0.09141	0.037094936	0.142523

Note. The total importance score of the pathway and the total score are 1, which is calculated based on the relative position of metabolites in the pathway; p value uncorrected: the enrichment significance of metabolite participation in the pathway; p value corrected: the corrected p value.

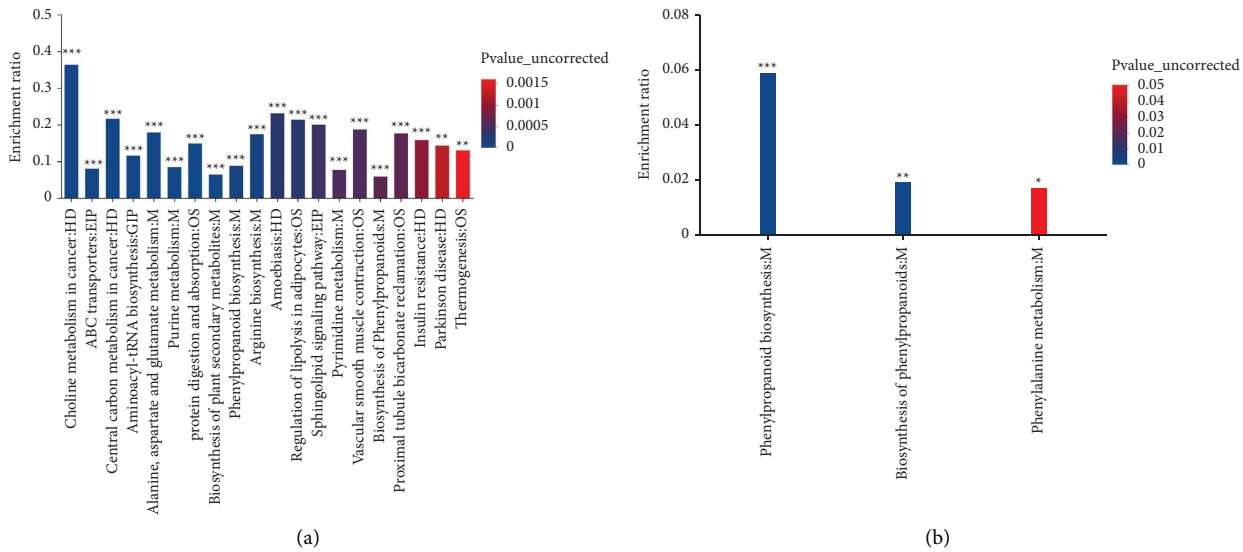

Figure 14: Enrichment analysis of the KEGG pathway. (a) The KEGG enrichment analysis graph. (b) KEGG topology analysis of bubble graphs.

state fermentation, the pH of fermentable can be kept stable with a good fermentation effect [46]. However, different fermentation substrates require different water contents, and the optimized water content of 55% in this experiment was favorable for the fermentation of *A. senticosus* to improve the polyphenol content. The appropriate fermentation temperature is an important factor affecting the growth and metabolism of the strain. Each microorganism has an optimum temperature for growth, and the mixed bacteria fermentation system also has an optimum temperature, below or above which the growth of microorganisms will be inhibited and the metabolic rate will be reduced. The results of this study showed that 37°C was the optimum temperature when *A. senticosus* had the best fermentation effect and the highest polyphenol content. A suitable inoculum level enables the strain to make full use of the substrate to react. A higher inoculum level may accelerate the growth rate of the strain, but at the same time, it will increase the rate of nutrient consumption. A very high inoculum level generates competition between strains that inhibit growth and reproduction, while a small inoculum level prolongs the time required for the fermentation process and leads to incomplete fermentation of the substrate. The results of this experiment showed that the inoculum level of 12.5% had the best fermentation effect.

Metabolomics is an emerging technology for comprehensively analyzing the changes in metabolites of the samples to be tested. It mainly analyzes and determines metabolites by high throughput measurement methods such as ultrahigh liquid chromatography-mass spectrometry and uses relevant databases combined with appropriate statistical methods to find out the different metabolites that perform biological functions of the samples to be tested, to analyze the reasons for their high active functions and lay the theoretical foundation for better utilization of biological resources [47]. Natural drugs contain many pharmacological components, but plant fibres prevent the precipitation of active ingredients [48]. Fermentation increases the digestion of plant fibers and enhances the content of active ingredients in natural drugs [49]. In this study, we performed a comprehensive analysis of *A. senticosus* before and after fermentation. By using nontargeted metabolomics techniques,

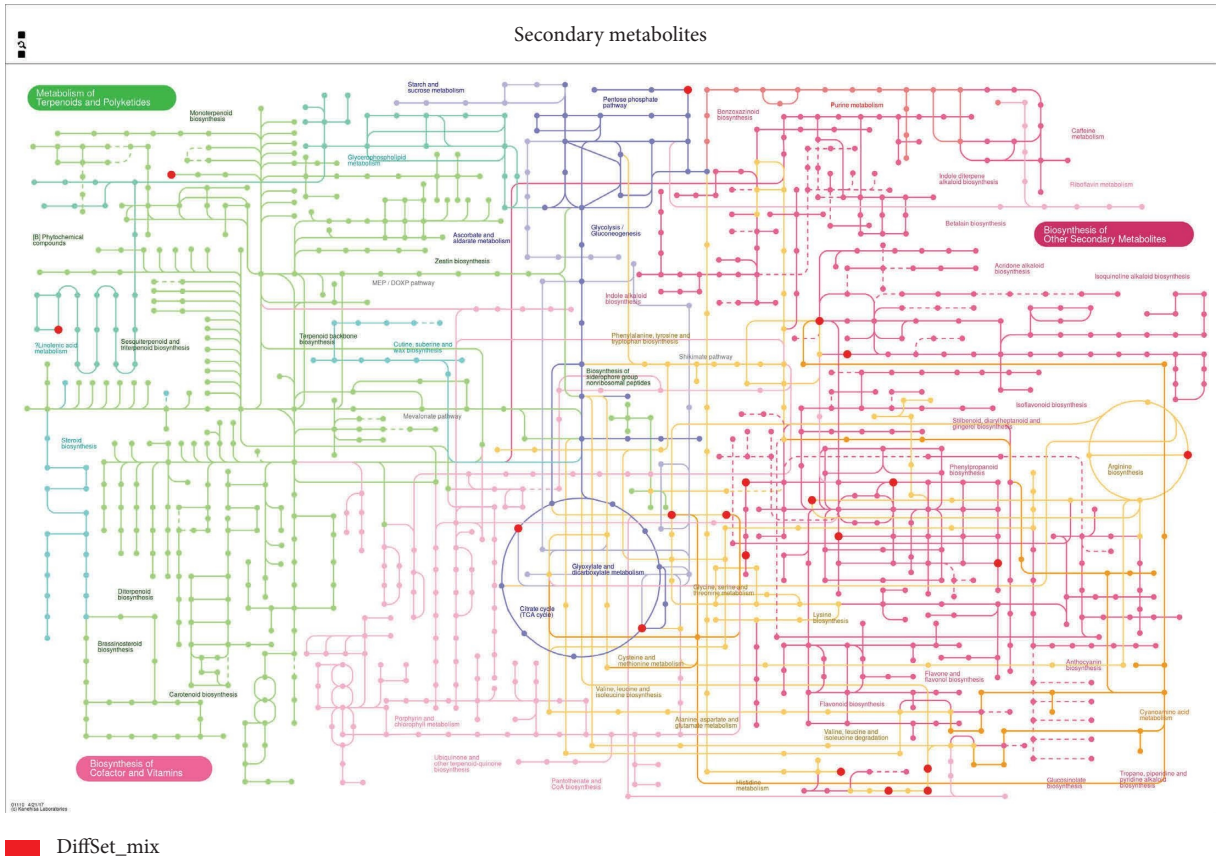

Figure 15: Metabolomics analysis in iPath.

we could not only quantify the known components but also identify the components by spectroscopy. The polyphenolic content and antioxidant activity of *A. senticosus* were enhanced before and after fermentation compared to those of *A. senticosus*.

Based on LC-MS untargeted metabolomics, we investigated the changes in metabolites before and after *A. senticosus* fermentation. We used LC-MS, univariate statistical analysis, and multivariate statistical analysis to investigate the distribution and patterns of metabolites before and after the fermentation of *A. senticosus*. PCA and PLS-DA analyses in the anion and cation modes of the samples before and after fermentation showed that the duplicate samples were relatively clustered within the group. The samples showed a clear separation trend among the groups. Through the construction and analysis of PCA, PLS-DA, and OPLS-DA models, a total of 601 secondary metabolites were identified in the anion and cation model and 238 different metabolites were identified before and after the fermentation of *A. senticosus*, mainly including lipids and lipid-like molecules, organic acids and derivatives, organic oxygen compounds, organoheterocyclic compounds, phenylpropanoids and polyketides, nucleosides, nucleotides, analog benzenoids, organic nitrogen compounds, alkaloids and derivatives, lignans, neolignans, and related compounds. The hierarchical clustering analysis of differential metabolites showed that the clustering of metabolites in both FAS and AS groups was divided into two major clusters, representing differential metabolites in AS before and after fermentation, with more than 60% differential metabolites with up-regulated expression compared to the unfermented group.

5. Conclusions

In this experiment, we used RSM to screen and optimize the optimal process for solid-state fermentation of *A. senticosus*: fermentation temperature of 37°C, fermentation time of 60 h, inoculum level of 12.5%, and water content of 55%. Under optimal conditions, the polyphenol content in *A. senticosus* was increased by 40% after fermentation. Subsequently, LC-MS untargeted metabolomic analysis was combined with multivariate analysis to systematically reveal the metabolic profile changes of *A. senticosus* during solid fermentation. A total of 601 major metabolic components were identified, 57 of which were phenolics. It was confirmed that probiotic fermentation had different effects on the content of secondary and primary metabolites of *A. senticosus*. This study further verified the feasibility and scientific validity of microbial fermentation of *A. senticosus*, theoretically supported that the active components and metabolites of *A. senticosus* changed significantly after fermentation, provided a new research strategy to elucidate the synergistic mechanism of microbial fermentation of *A. senticosus*, and offered new research ideas for the comprehensive development and utilization of *A. senticosus*.

Data Availability

The data sets used and/or analyzed during the present study are available from the corresponding author upon reasonable request.

Disclosure

Jianqing Su and Xiang Fu are the co-first authors.

Conflicts of Interest

The authors declare that there are no conflicts of interest.

Authors' Contributions

Xiang Fu prepared the original draft, wrote and edited the review, visualized the study, and curated the data. Rui Zhang was involved in the methodology. Xiaoli Li investigated the study. Ying Li performed the formal analysis. Jianqing Su acquired funding and supervised the study. Xiuling Chu conceptualized the study and managed the resources. All authors have read and agreed to the published version of the manuscript. Jianqing Su and Xiang Fu contributed equally to this work.

Acknowledgments

The authors gratefully acknowledge the financial support provided by the National Natural Science Foundation, China (Grant nos. 31872515and 32172901).

References

[1] T. Li, K. Ferns, Z. Q. Yan et al., "Acanthopanax senticosus: photochemistry and anticancer potential," *American Journal of Chinese Medicine*, vol. 44, no. 8, pp. 1543–1558, 2016.

[2] X. Gu, G. Zhang, Q. Wang et al., "Integrated network pharmacology and hepatic metabolomics to reveal the mechanism of Acanthopanax senticosus against major depressive disorder," *Frontiers in Cell and Developmental Biology*, vol. 10, Article ID 900637, 2022.

[3] D. Załuski and H. D. Smolarz, "TLC profiling, nutritional and pharmacological properties of Siberian ginseng (Eleutherococcus senticosus) cultivated in Poland," *Pakistan journal of pharmaceutical sciences*, vol. 29, no. 5, pp. 1497–1502, 2016.

[4] Y. Han, A. Zhang, H. Sun et al., "High-throughput ultra high performance liquid chromatography combined with mass spectrometry approach for the rapid analysis and characterization of multiple constituents of the fruit of*Acanthopanax senticosus*(Rupr. et Maxim.) Harms," *Journal of Separation Science*, vol. 40, no. 10, pp. 2178–2187, 2017.

[5] F. Li, W. Li, H. Fu, Q. Zhang, and K. Koike, "Pancreatic lipase-inhibiting triterpenoid saponins from fruits of Acanthopanax senticosus," *Chemical and Pharmaceutical Bulletin*, vol. 55, no. 7, pp. 1087–1089, 2007.

[6] H. Gao, W. Xu, Y. H. Zhang, Z. D. Qiu, C. M. Fu, and X. N. Qi, "Anti-fatigue mechanism of acanthopanax senticosus glycosides based on network pharmacologychinese traditional and herbal drugs," *Phytother Res*, vol. 52, no. 2, pp. 413–421, 2021.

[7] X. L. Zhang, F. Ren, W. Huang, R. T. Ding, Q. S. Zhou, and X. W. Liu, "Anti-fatigue activity of extracts of stem bark from Acanthopanax senticosus," *Molecules*, vol. 16, no. 1, pp. 28–37, 2010.

[8] A. Ganogpichayagrai and C. Suksaard, "Proximate composition, vitamin and mineral composition, antioxidant capacity, and anticancer activity of Acanthopanax trifoliatus," *Journal of Advanced Pharmaceutical Technology & Research*, vol. 11, no. 4, pp. 179–183, 2020.

[9] Z. Chen, S. Cheng, H. Lin et al., "Antibacterial, anti-inflammatory, analgesic, and hemostatic activities of Acanthopanax trifoliatus (L.) merr," *Food Science and Nutrition*, vol. 9, no. 4, pp. 2191–2202, 2021.

[10] D. Plamada and D. C. Vodnar, "Polyphenols-Gut microbiota interrelationship: a transition to a new generation of prebiotics," *Nutrients*, vol. 14, no. 1, p. 137, 2021.

[11] X. Chen, M. Ishfaq, and J. Wang, "Effects of Lactobacillus salivarius supplementation on the growth performance, liver function, meat quality, immune responses and Salmonella Pullorum infection resistance of broilers challenged with Aflatoxin B1," *Poultry Science*, vol. 101, no. 3, Article ID 101651, 2022.

[12] Y. H. Jiang, W. G. Xin, L. Y. Yang et al., "A novel bacteriocin against *Staphylococcus aureus* from Lactobacillus paracasei isolated from Yunnan traditional fermented yogurt: purification, antibacterial characterization, and antibiofilm activity," *Journal of Dairy Science*, vol. 105, no. 3, pp. 2094–2107, 2022.

[13] S. Hang, L. Zeng, J. Han et al., "Lactobacillus plantarum ZJ316 improves the quality of Stachys sieboldii Miq. pickle by inhibiting harmful bacteria growth, degrading nitrite and promoting the gut microbiota health in vitro," *Food & Function*, vol. 13, no. 3, pp. 1551–1562, 2022.

[14] F. Q. Fu, M. Xu, Z. Wei, and W. Li, "Biostudy on traditional Chinese medicine massa medicata fermentata," *ACS Omega*, vol. 5, no. 19, pp. 10987–10994, 2020.

[15] L. Li, L. Wang, W. Fan et al., "The application of fermentation technology in traditional Chinese medicine: a review," *American Journal of Chinese Medicine*, vol. 48, no. 4, pp. 899–921, 2020.

[16] Y. Lu and J. G. Jiang, "Application of enzymatic method in the extraction and transformation of natural botanical active ingredients," *Applied Biochemistry and Biotechnology*, vol. 169, no. 3, pp. 923–940, 2013.

[17] X. Zhang, A. Rogowski, L. Zhao et al., "Understanding how the complex molecular architecture of mannan-degrading hydrolases contributes to plant cell wall degradation," *Journal of Biological Chemistry*, vol. 289, no. 4, pp. 2002–2012, 2014.

[18] Z. H. Pu, M. Dai, L. Xiong, and C. Peng, "Total alkaloids from the rhizomes of Ligusticum striatum: a review of chemical analysis and pharmacological activities," *Natural Product Research*, vol. 36, no. 13, pp. 3489–3506, 2022.

[19] R. Temmar, M. Rodríguez-Prado, G. Forgeard, C. Rougier, and S. Calsamiglia, "Interactions among natural active ingredients to improve the efficiency of rumen fermentation in vitro," *Animals*, vol. 11, no. 5, p. 1205, 2021.

[20] M. E. P. Papadimitropoulos, C. G. Vasilopoulou, C. Maga-Nteve, and M. I. Klapa, "Untargeted GC-MS metabolomics," *Methods in Molecular Biology*, vol. 1738, pp. 133–147, 2018.

[21] A. Di Minno, M. Gelzo, M. Stornaiuolo, M. Ruoppolo, and G. Castaldo, "The evolving landscape of untargeted metabolomics," *Nutrition, Metabolism, and Cardiovascular Diseases*, vol. 31, no. 6, pp. 1645–1652, 2021.

[22] D. D. Zhou, A. Saimaiti, M. Luo et al., "Fermentation with tea residues enhances antioxidant activities and polyphenol

contents in kombucha beverages," *Antioxidants*, vol. 11, no. 1, p. 155, 2022.

[23] H. N. T. Pham, V. T. Nguyen, Q. Vuong, M. C. Bowyer, and C. J. Scarlett, "Effect of extraction solvents and drying methods on the physicochemical and antioxidant properties of helicteres hirsuta lour. Leaves," *Technologies*, vol. 3, no. 4, pp. 285–301, 2015.

[24] W. Brand-Williams, M. E. Cuvelier, and C. Berset, "Use of a free radical method to evaluate antioxidant activity," vol. 28, no. 1, pp. 25–30, 1995.

[25] K. Thaipong, U. Boonprakob, K. Crosby, L. Cisneros-Zevallos, and D. Hawkins Byrne, "Comparison of ABTS, DPPH, FRAP, and ORAC assays for estimating antioxidant activity from guava fruit extracts," *Journal of Food Composition and Analysis*, vol. 19, no. 6-7, pp. 669–675, 2006.

[26] A. M. Abdel-Aty, R. I. Bassuiny, A. Z. Barakat, and S. A. Mohamed, "Upgrading the phenolic content, antioxidant and antimicrobial activities of garden cress seeds using solid-state fermentation by Trichoderma reesei," *Journal of Applied Microbiology*, vol. 127, no. 5, pp. 1454–1467, 2019.

[27] J. R. Williams, R. Yang, J. L. Clifford et al., "Functional Heatmap: an automated and interactive pattern recognition tool to integrate time with multi-omics assays," *BMC Bioinformatics*, vol. 20, no. 1, p. 81, 2019.

[28] K. Ben Salem and A. Ben Abdelaziz, "Principal component analysis (PCA)," *Tunisie Medicale*, vol. 99, no. 4, pp. 383–389, 2021.

[29] L. C. Lee and A. A. Jemain, "Predictive modelling of colossal ATR-FTIR spectral data using PLS-DA: empirical differences between PLS1-DA and PLS2-DA algorithms," *Analyst*, vol. 144, no. 8, pp. 2670–2678, 2019.

[30] Z. Xu, Y. Sheng, G. Zeng et al., "Metabonomic study on the plasma of high-fat diet-induced dyslipidemia rats treated with Ge gen qin lian decoction by ultrahigh-performance liquid chromatography-mass spectrometry," *Evidence-based Complementary and Alternative Medicine*, vol. 2021, Article ID 6692456, 16 pages, 2021.

[31] P. D. Karp, N. Ivanova, M. Krummenacker et al., "A comparison of microbial genome web portals," *Frontiers in Microbiology*, vol. 10, p. 208, 2019.

[32] A. Ishizaki and H. Kataoka, "Online in-tube solid-phase microextraction coupled to liquid chromatography-tandem mass spectrometry for the determination of tobacco-specific nitrosamines in hair samples," *Molecules*, vol. 26, no. 7, p. 2056, 2021.

[33] D. Kumar, R. Joshi, A. Sharma, G. Nadda, and D. Kumar, "A comprehensive search of the primary and secondary metabolites and radical scavenging potential of trillium govanianum wall. Ex D. Don," *Chemistry and Biodiversity*, vol. 18, no. 10, Article ID 2100300, 2021.

[34] S. H. Yoon, E. Koh, B. Choi, and B. Moon, "Effects of soaking and fermentation time on biogenic amines content of maesil (prunus mume) extract," *Foods*, vol. 8, no. 11, p. 592, 2019.

[35] Q. Liu, W. Zhong, X. Yang et al., "Study on screening of fermentation agents and optimization of the fermentation process for pharyngitis tablet residue," *Frontiers in Veterinary Science*, vol. 9, Article ID 981388, 2022.

[36] J. Wang, F. Cao, E. Su, L. Zhao, and W. Qin, "Improvement of animal feed additives of ginkgo leaves through solid-state fermentation using Aspergillus Niger," *International Journal of Biological Sciences*, vol. 14, no. 7, pp. 736–747, 2018.

[37] X. Liu, X. Gao, R. Zhang et al., "Discovery and comparison of serum biomarkers for diabetes mellitus and metabolic syndrome based on UPLC-Q-TOF/MS," *Clinical Biochemistry*, vol. 82, pp. 40–50, 2020.

[38] K. K. Oh, M. Adnan, and D. H. Cho, "Active ingredients and mechanisms of Phellinus linteus (grown on Rosa multiflora) for alleviation of Type 2 diabetes mellitus through network pharmacology," *Gene*, vol. 768, Article ID 145320, 2021.

[39] R. Liu, X. Chu, J. Su et al., "Enzyme-assisted ultrasonic extraction of total flavonoids from Acanthopanax senticosus and their enrichment and antioxidant properties," *Processes*, vol. 9, no. 10, p. 1708, 2021.

[40] Q. Qu, F. Yang, C. Zhao et al., "Effects of fermented ginseng on the gut microbiota and immunity of rats with antibiotic-associated diarrhea," *Journal of Ethnopharmacology*, vol. 267, Article ID 113594, 2021.

[41] P. Huang, P. Wang, J. Xu et al., "Fermented traditional Chinese medicine alters the intestinal microbiota composition of broiler chickens," *Research in Veterinary Science*, vol. 135, pp. 8–14, 2021.

[42] X. Guo, Z. Yan, J. Wang et al., "Effect of traditional Chinese medicine (TCM) and its fermentation using Lactobacillus plantarum on ceftriaxone sodium-induced dysbacteriotic diarrhea in mice," *Chinese Medicine*, vol. 17, no. 1, p. 20, 2022.

[43] S. Liu, W. Yan, C. Ma et al., "Effects of supplemented culture media from solid-state fermented Isaria cicadae on performance, serum biochemical parameters, serum immune indexes, antioxidant capacity and meat quality of broiler chickens," *Asian-Australasian Journal of Animal Sciences*, vol. 33, no. 4, pp. 568–578, 2020.

[44] J. Gao, R. Wang, J. Liu, W. Wang, Y. Chen, and W. Cai, "Effects of novel microecologics combined with traditional Chinese medicine and probiotics on growth performance and health of broilers," *Poultry Science*, vol. 101, no. 2, Article ID 101412, 2022.

[45] D. Kumar, M. K. Lal, S. Dutt et al., "Functional fermented probiotics, prebiotics, and synbiotics from non-dairy products: a perspective from nutraceutical," *Molecular Nutrition & Food Research*, vol. 66, no. 14, Article ID 2101059, 2022.

[46] H. Lee, S. Lee, S. Kyung et al., "Metabolite profiling and anti-aging activity of rice koji fermented with Aspergillus oryzae and Aspergillus cristatus: a comparative study," *Metabolites*, vol. 11, no. 8, p. 524, 2021.

[47] C. P. Sreena and D. Sebastian, "Augmented cellulase production by Bacillus subtilis strain MU S1 using different statistical experimental designs," *Journal of Genetic Engineering and Biotechnology*, vol. 16, no. 1, pp. 9–16, 2018.

[48] Q. Xu, Q. Qiao, Y. Gao et al., "Gut microbiota and their role in health and metabolic disease of dairy cow," *Frontiers in Nutrition*, vol. 8, Article ID 701511, 2021.

[49] S. Yuan, C. Y. Xu, J. Xia, Y. N. Feng, X. F. Zhang, and Y. Y. Yan, "Extraction of polysaccharides from Codonopsis pilosula by fermentation with response surface methodology," *Food Science and Nutrition*, vol. 8, no. 12, pp. 6660–6669, 2020.